Universidade de Lisboa

Faculdade de Medicina de Lisboa

Contribution of different cellular subsets to the Adenosine A_{2A} Receptor overexpression in the rat brain

Ana Inês Marques Morgado

Mestrado em Neurociências

Dissertação

Março de 2016

Universidade de Lisboa

Faculdade de Medicina de Lisboa

Contribution of different cellular subsets to the Adenosine A_{2A} Receptor overexpression in the rat brain

Ana Inês Marques Morgado

Dissertação orientada por:

Doutora Joana E. Coelho

Doutora Luísa V. Lopes

Mestrado em Neurociências

Dissertação

Março de 2016

Todas as afirmações efetuadas no presente documento são da exclusiva responsabilidade da sua autora, não cabendo qualquer responsabilidade à Faculdade de Medicina de Lisboa pelos conteúdos nele apresentados.

A impressão desta dissertação foi aprovada pelo Conselho Científico da Faculdade de Medicina de Lisboa em reunião de 19 de abril de 2016

RESUMO

O Sistema Nervoso Central caracteriza-se por uma organização estrutural em sinapses multipartidas, constituídas por diversos tipos celulares que coexistem em contínua inter-relação, estabelecendo a base funcional da homeostasia.

A Adenosina, ao ser um metabolito presente em todos os subtipos celulares, ganha relevância pela sua capacidade de modular a função cerebral através de acções a nível da transmissão sináptica – regulando a libertação de neurotransmissores, excitabilidade pós-sináptica e resposta de vários tipos de receptores – e da fisiologia das células gliais. Esta modulação homeostática é mediada pela acção de quatro receptores pleiotrópicos (A_1, A_{2A}, A_{2B} and A_3) que activam diferentes vias de transdução, de acordo com o seu grau de activação e localização celular e subcelular. Particularmente a nível do hipocampo, a acção deste importante neuromodulador resulta de um balanço entre as respostas inibitórias dos receptores A_1 e os efeitos facilitadores da activação dos receptores A_{2A}.

Os receptores A_{2A} são receptores metabotrópicos excitatórios que, apesar de pouco expressos a nível do hipocampo, actuam como metamoduladores da actividade sináptica, através da regulação da libertação de glutamato, GABA e acetilcolina, aliada à interacção com diversos receptores de neuromoduladores, neurotransmissores e neurotrofinas. Além do controlo da função neuronal, as suas acções estendem-se à função dos astrócitos e da microglia, ocupando uma posição de destaque na modulação das relações funcionais entre diversos tipos celulares.

Diversos estudos relacionam situações de insulto - tais como stress, epilepsia, hipoxia, isquémia e envelhecimento – caracterizadas por um aumento extracelular da concentração de adenosina, com a indução de uma desregulação do sistema adenosinérgico, devido à sobreexpressão de receptores A_{2A} a nível do córtex e hipocampo, levando a fenómenos de excitotoxicidade, retracção dendrítica e alterações da memória e plasticidade sináptica. Embora o mecanismo subjacente a esta sobreexpressão patológica permaneça desconhecido, bem como o subtipo neuronal directamente afectado, sabe-se que este tipo de situações prejudiciais à fisiologia do sistema nervoso induzem alterações que seguem a mesma tendência daquelas que ocorrem com o envelhecimento.

De forma a permitir o estudo da desregulação destes receptores no hipocampo, foi criado um modelo de ratos transgénicos que sobreexpressa o subtipo humano do receptor A_{2A} sob o controlo do promotor da proteína cinase dependente de cálcio/calmodulina (Tg(CaMKII-hA_{2A}R)), permitindo uma sobreexpressão pós-natal a nível dos neurónios do prosencéfalo, que mimetiza o processo patológico decorrente de circunstâncias de insulto. Sabendo que estes animais apresentam alterações semelhantes às do envelhecimento, com consequências a nível cognitivo, sináptico e molecular, o presente estudo teve como objectivo avaliar a contribuição de diversos subtipos celulares para este comprometimento da função do hipocampo.

Em primeiro lugar, de forma a abordar as consequências desta sobrexpressão a nível dos circuitos neuronais do hipocampo, foram efectuadas diversas técnicas de biologia molecular para caracterizar a sua localização neste modelo transgénico, tendo sido confirmado através de imunohistoquímica que estes animais expressam o receptor A_{2A} humano nas projecções axonais de CA3 e a nível de CA1 e do Girus Dentado.

Após esta caracterização, avaliou-se se as alterações induzidas no hipocampo estariam relacionadas com perda neuronal ou modificações na densidade sináptica. Não foram encontradas diferenças significativas no número de neurónios da camada piramidal de CA1 nem nos níveis proteicos de marcadores de densidade sináptica (PSD-95 e SNAP-25) no hipocampo de animais Tg(CaMKII-hA_{2A}R) e WT.

A segunda parte do estudo consistiu na avaliação de possíveis alterações a nível do fenótipo das células da microglia e dos astrócitos, explorando a sua contribuição para o processo patológico.

Procedeu-se à caracterização do fenótipo das células da microglia, através de uma abordagem combinada de *Western Blotting*, imunohistoquímica e citometria de fluxo. Paralelamente a um aumento significativo de 66.91 ± 24.77% dos níveis proteicos de Iba1 no hipocampo de animais transgénicos, foram encontradas diferenças morfológicas significativas relativas à diminuição da área de influência celular ($4{,}64x10^8$ ± $5{,}134x10^7$ μm^2) e à aquisição de uma morfologia menos arredondada da microglia na região de CA1 de animais transgénicos, comparativamente aos WT. No entanto, não foram encontradas diferenças significativas em relação ao número de células microgliais e aos níveis de expressão de CD11b.

Os resultados obtidos demonstram que a sobreexpressão neuronal de receptores A_{2A} é suficiente para desencadear alterações ao nível do fenótipo da microglia, semelhantes às que caracterizam as fases iniciais do seu processo de activação. A existência de um estado crónico de activação da microglia pode levar ao estabelecimento de um ambiente pró-inflamatório, devido à libertação de citocinas e mediadores inflamatórios, com possível contribuição para as alterações verificadas ao nível da plasticidade sináptica do hipocampo neste modelo transgénico.

Por fim, procedeu-se à caracterização do fenótipo dos astrócitos, através de *Western Blotting* e imunohistoquímica. Observou-se uma diminuição da reactividade dos astrócitos, pela diminuição significativa de 20.76 ± 8.019% dos níveis de GFAP no hipocampo de animais transgénicos comparativamente aos WT. No que diz respeito à análise morfológica destas células, não foram encontradas diferenças significativas na densidade, distribuição e morfologia dos astrócitos da região de CA1 entre animais transgénicos e WT.

A sobreexpressão de receptores A_{2A} a nível neuronal induz uma diminuição de reactividade dos astrócitos, consistente com um fenótipo de astenia. A perda de função dos astrócitos é uma característica importante do processo de neurodegeneração, com prejuízo da função neuronal resultante de um desajuste homeostático, nomeadamente ao nível da disfunção dos

transportadores de glutamato. Diminuições dos níveis de GFAP estão também correlacionadas com patologia depressiva em humanos e modelos animais, o que é consistente com as características depressivas presentes neste modelo de sobreexpressão de receptores A_{2A} previamente analisadas através de estudos comportamentais. Assim, as alterações verificadas ao nível sináptico e comportamental nos animais transgénicos podem em parte ser explicadas por uma alteração da função dos astrócitos.

O presente trabalho comprova que a sobreexpressão de receptores A_{2A} em neurónios é suficiente para induzir alterações significativas ao nível da função das células gliais. Deste modo, as consequências cognitivas, sinápticas e moleculares que decorrem da desregulação dos receptores $A_{2A}R$ no hipocampo, em contextos de insulto para a fisiologia do sistema nervoso, derivam de uma desregulação conjunta de células neuronais e gliais, num mecanismo semelhante ao do envelhecimento.

Para além de contribuir para melhorar o conhecimento sobre os processos neuropatológicos, este estudo reforça a necessidade de considerar a neurodegeneração como uma consequência da perda de homeostasia, dando igual relevância à contribuição das alterações funcionais, celulares e moleculares a nível neuronal e das células da glia.

Palavras-chave: Adenosina; receptor A_{2A}; neurodegeneração; microglia, astrócitos, hipocampo; sinapse

ABSTRACT

Adenosine A_{2A} receptors ($A_{2A}R$) are excitatory metabotropic receptors that act as metamodulators of synaptic activity in the hippocampus, by influencing the release/uptake of glutamate, GABA and acetylcholine together with the interaction with receptors for other neuromodulators, neurotransmitters and neurotrophic factors and the modulation of glial cell function.

Noxious brain conditions, such as stress and aging, are known to induce a dysregulation of adenosinergic system characterized by long-term robust upregulation of $A_{2A}R$ in cortical and hippocampal regions, leading to an imbalance of the overall effect of adenosine with excitotoxixity phenomena, dendritic retraction and memory and synaptic plasticity impairment. Although little is known on the mechanism involved in this $A_{2A}R$ upsurge, different studies have found common features between this type of dysregulation and those found in aged animals, raising an early-aging hypothesis behind neurodegeneration.

In order to clarify the involvement of different cellular subsets in the $A_{2A}R$ hippocampal dysregulation, we characterized glial cell phenotype in a model of transgenic rats with a postnatal overexpression of human $A_{2A}R$ conditional to the glutamatergic forebrain neurons (Tg(CaMKII-h$A_{2A}R$)) that displays age-like alterations in hippocampal function, with cognitive, synaptic and molecular impairments.

We found that human $A_{2A}R$ overexpression in forebrain neurons is sufficient to drive significant changes in glial cell function, inducing a primed state of microglia – triggering morphological alterations that resemble early states of activation process – and an asthenic phenotype of astrocytes by decreasing GFAP expression. Therefore, the pathological process of $A_{2A}R$ dysregulation derives from a synergy of synaptic and glial dysfunction that resembles features of hippocampal aging.

By highlighting the importance of considering neurodegeneration as a consequence of homeostatic failure, results give relevance to the molecular and cellular changes in glia as well as neurons, when trying to decipher the mechanisms leading to neuropathology, suggesting $A_{2A}R$ as a promising multifactorial tool of therapeutic interest.

Key Words: Adenosine A_{2A} receptor; overexpression; neurodegeneration; microglia; astrocyte; hippocampus; multipartite synapse; microglial activation; astroglial asthenia.

INDEX

FIGURE INDEX

TABLE INDEX

LIST OF ABBREVIATIONS

A_1R Adenosine A_1 Receptor

$A_{2A}R$ Adenosine A_{2A} Receptor

AC Adenylate Cyclase

AD Alzheimer's Disease

AMPA α-amino-3-hydroxy-5-methyl-4-isoxazolepropionic acid

ANOVA Analysis of Variation

ATP Adenosine Triphosphate

BDNF Brain Derived Neurotrophic Factor

bp Base Pairs

BSA Bovine Serum Albumin

BW Body Weight

CA *Cornu Ammonis*

CaMKII Ca^{2+}/calmodulin-dependent protein kinase II

CD Cluster of Differentiation

CNS Central Nervous System

DAB 3,3'-Diaminobenzidine

DG Dentate Gyrus

dH2O Distilled water

DMEM Dulbecco's Modified Eagle Medium

DNA Deoxyribonucleic Acid

DTT 1,4-dithiothreitol

EAAT1 Excitatory Amino Acid Transporter 1

EAAT2 Excitatory Amino Acid Transporter 2

FBS Fetal Bovine Serum

FITC Fluorescein isothiocyanate

GABA γ-Aminobutyric acid

GAPDH Glyceraldehyde 3-Phosphate Dehydrogenase

GFAP Glial Fibrillary Acidic Protein

HBSS Hanks' Balanced Salt Solution

Iba1 Ionized Calcium-Binding Adapter Molecule 1

IL Interleukin

LPS Lipopolysaccharide

LTD Long-Term Depression

LTP Long-Term Potentiation

MAP-2 Microtubule-associated protein 2

MAPK Mitogen Activated Protein Kinase

MHC Major Histocompatibility Complex

NMDA N-Methyl-D-aspartate

NO Nitric Oxide

PCR Polymerase Chain Reaction

PD Parkinson's Disease

PE Phycoerythrin

PFA Paraformaldehyde

PIPES Piperazine-N,N′-bis(2-ethanesulfonic acid)

PKA Protein Kinase A

PKC Protein Kinase C

PSD-95 Postsynaptic Density Protein 95

PVDF Polyvinylidene Fluoride

RIPA Radio-Immunoprecipitation Assay

SDS Sodium Dodecyl Sulphate

SDS-PAGE Sodium Dodecyl Sulphate - Polyacrylamide Gel Electrophoresis

SEM Standard Error of the Mean

SNAP-25 Synaptosomal-associated protein 25

SYP Synaptophysin

TBS Tris Buffered Saline

Tg Transgenic

Tg(CaMKII-hA_{2A}R) Transgenic rat model that overexpresses human A_{2A}R driven by the CaMKIIα promoter

TGF Transforming Growth Factor

TNF Tumor Necrosis Factor

WT Wildtype

1 | INTRODUCTION

1.1 | Adenosine: coordinator of brain function

Adenosine is a purine nucleoside produced through the catabolism of ATP by ecto-nucleotidases. Ubiquitously present in all cell types, its ability to modulate cell metabolism is widely described, namely in Central Nervous System (CNS), where it is considered a homeostatic coordinator of brain function, able to influence synaptic transmission, triggering or braking the activity of different neurotransmitters and neuromodulators (Ribeiro & Sebastião, 2010). Accordingly, adenosinergic system is responsible for the control of the flow of information rather than its transmission, regulating neurotransmitter release, post-synaptic excitability and the response of several brain receptors (Cunha, 2005; Sebastiao & Ribeiro, 2009). Moreover, this modulatory potential is also extended to astrocytes, microglia and oligodendrocytes, being well positioned to mediate neuron-glia communication (Daré et al., 2007).

The neuromodulatory role of adenosine is mediated by four pleiotropic receptors -– A_1, A_{2A}, A_{2B} and A_3 – that couple to different G proteins, activating different transducing pathways according to their degree of activation and cellular and sub-cellular localization. Nonetheless, the impact of adenosine on brain function is mostly defined by a dynamic balance between the inhibitory and excitatory actions of A_1 and A_{2A} receptors, respectively. In fact, the differential activation of these receptors with opposing outcomes consists of a function of the activity of nerve terminals, with the effects of A_1 receptors predominating at low frequencies of stimulation and a preferential activation of A_{2A} receptors following high frequencies (Cunha, 2005). Although A_1 and A_{2A} receptors are widespread in the CNS, their relative proportions differ greatly according to the brain region. While A_1 receptors are more abundant in the cortex, cerebellum and hippocampus, A_{2A} display a more restricted expression pattern with high density in basal ganglia (Ribeiro et al., 2003).

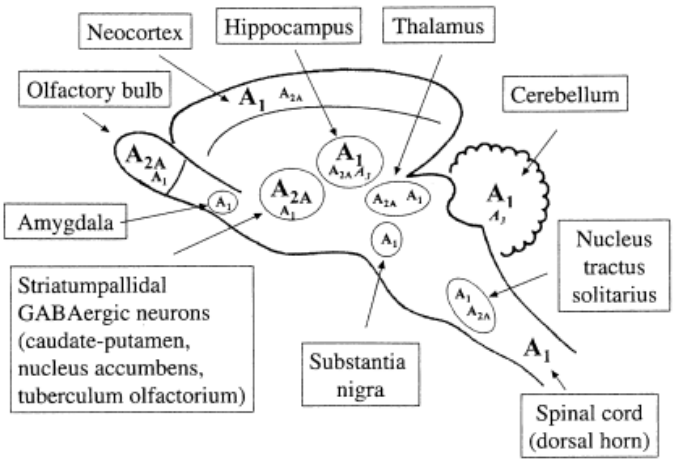

Figure 1.1 - Schematic representation of the distribution of adenosine receptors in the brain.

The hippocampus presents high levels of A_1R and low levels of A_{2A}R (from Ribeiro et al., 2003)

1.2 | $A_{2A}R$ in hippocampal physiology and disease

In spite of their low density in the hippocampus, with predominant presynaptic localization, A_{2A} receptors ($A_{2A}R$) play an important role in the modulation of synaptic transmission, not restricted to the control of neuronal function but also through their impact on astrocytic and microglial function.

The metamodulator properties of $A_{2A}R$ reflect their ability to facilitate the release of most neurotransmitter types, along with their regulation of the function of metabotropic, ionotropic and catalytic receptors of other modulatory systems (Sebastiao & Ribeiro, 2009; Ribeiro & Sebastião, 2010). Pre-synaptically, $A_{2A}R$ activation modulates the release or uptake of glutamate, acetylcholine and GABA (Cunha, 2005). In glutamatergic terminals, these receptors possess release-regulating properties, leading to facilitation of glutamate release and synaptic transmission, through different mechanisms, such as: (1) a cross-talk with A_1 receptors (A_1R)– decreasing their binding affinity and tonic inhibition, in a manner dependent on intracellular transduction (Lopes et al., 2002); (2) promoting K+-evoked glutamate release (Marcoli et al., 2003), and by (3) a synergistic interaction with mGlu5 receptors, enhancing their responses (Tebano et al., 2006). Moreover, their activation of Adenylate Cyclase/Protein Kinase A (AC/PKA) pathway has effects on cholinergic and GABAergic transmission, promoting acetylcholine release (Rebola et al., 2002) and enhanced GAT-1 mediated GABA transport into nerve endings (Cristóvão-Ferreira et al., 2009). Furthermore, at post-synaptic level, $A_{2A}R$ interact and modulate the activity of different types of receptors, namely enhancing AMPA receptors-evoked currents and facilitating NMDA receptor functioning (Ribeiro & Sebastião, 2010; Sebastiao & Ribeiro, 2009). Additionally, their activation is a crucial requisite for the functioning of neurotrophic receptors, being able to transactivate TrkB receptors in the absence of Brain Derived Neurotrophic Factor (BDNF) (Lee & Chao, 2001). On the other hand, as $A_{2A}R$ are pleiotropic receptors it is also important to highlight their ability to signal through PKA-independent pathways, including PKC (R. A. Cunha & Ribeiro, 2000), MAPK (Schulte & Fredholm, 2003), β-arrestin (Khoa et al., 2006) and Src-TrkA (Malek et al., 1999) as well as to bind to several interacting proteins, which can complement and modulate their G-protein-dependent function (Fredholm et al., 2007).

These complex interactions may justify the apparent paradoxical effects of these receptors. In fact, while $A_{2A}R$ activation was reported to play a protective role in cases of intracerebral hemorrhage, hippocampal kainate-induced excitotoxicity, striatal lesion and spinal cord injury, strategies of genetic and pharmacological inactivation of the same receptor have been proven to afford neuroprotection in contexts of dopaminergic neurodegeneration, excitoxicity, β-amyloid aggregation and traumatic brain injury, as well as to reduce cognitive impairment and decrease Aβ levels in the brain of transgenic mouse models of Alzheimer's Disease (AD) (reviewed in Dai et al., 2010).

Noteworthy, extracellular adenosine and glutamate levels rise rapidly and dramatically in response to brain insults, due to increased ATP release and altered glutamate presynaptic neuronal release/ astrocytic reversal uptake, respectively. Higher levels of adenosine activate preferentially $A_{2A}R$ and

cause A_1R desensitization, favouring glutamate release (Cunha, 2005). Thus, this interplay between adenosine and glutamate levels defines the functional outcome of $A_{2A}R$, being responsible for a feedforward loop that leads to neurodegeneration. Therefore, this dual neuroprotective potential of $A_{2A}R$ modulation seems to be dependent on the specific profile of the pathology and the stage of the pathological where the exposure to agonists or antagonists occurs (Dai et al., 2010).

In fact, although tonic inhibitory activity of A_1R counteracts $A_{2A}R$ facilitatory effects at physiological state (Lopes et al., 2002), different noxious brain conditions - such as hypoxia, ischemia, epilepsy, stress or aging - in which there is a modification of the extracellular metabolism of adenosine, are related to a decrease in expression and density of A_1R and a long term robust upregulation of $A_{2A}R$ in cortical and hippocampal regions. This imbalance of the overall effect of adenosine causes greater susceptibility of brain tissue to stressful stimuli and neuronal damage, leading to excitotoxicity, dendritic retraction and memory and synaptic plasticity impairment (Cunha, 2005; Batalha et al., 2013). Accordingly, it was shown that in aged animals, $A_{2A}R$-dependent glutamate release becomes more pronounced and shifts from a PKC-mediated signalling to a PKA-dependent effect (Lopes et al., 1999), which is accompanied with behavioural deficits in hippocampal-dependent tasks (Diógenes et al., 2011).

Nonetheless, the mechanism involved in this $A_{2A}R$ upsurge and which exactly are the neurotransmitters or neuronal pool directly affected are yet unknown. This process can be seen as a result of a physiological stress condition, being a compensatory mechanism to offset the loss of efficiency of functioning of brain circuits (Rosenzweig & Barnes, 2003), namely through the increase of acetylcholine release. However, this could also result in excitotoxicity phenomena, by the promotion of glutamate release and GABA transmission, which could lead to the inhibition of hippocampal interneurons, thereby reinforcing glutamatergic action. Nevertheless, it is interesting to notice that this changes concerning adenosine receptor system in aged animals are similar to that found on noxious brain conditions, which rises an early-aging hypothesis behind neurodegeneration (Cunha, 2005; Batalha et al., 2013).

1.3 | Rat Model of $A_{2A}R$ Overexpression (Tg(CaMKII-h$A_{2A}R$))

In order to overcome current limitations that difficult proper investigation on the dysregulation of hippocampal $A_{2A}R$ function, transgenic rats that overexpress human $A_{2A}R$ driven by the CaMKIIα promoter have been generated (Tg(CaMKII-h$A_{2A}R$)). The latter allows a profile of postnatal overexpression conditional to the glutamatergic forebrain neurons – mainly in the hippocampus and cortex – having very restricted expression in other areas (Coelho et al., 2014), with protein levels that are comparable to that found in physiological aging, without affecting A_1R levels.

Consequently, this animal model displays age-like alterations in hippocampal function, with cognitive, synaptic and molecular impairments. At the synaptic level, an increase in neuronal $A_{2A}R$

is sufficient to increase glutamate release probability and intracellular Ca^{2+} levels, as well as to enhance synaptic NMDAR currents and decrease AMPAR currents, causing a shift in LTP/LTD probability (Temido-Ferreira et al., 2015). Accordingly, these alterations in synaptic function drive an impairment in hippocampal-dependent tasks both in spatial memory and short-term reference memory.

All gathered, these features and their reversal by blocking $A_{2A}R$ activation strongly support the hypothesis that $A_{2A}R$ dysregulation drives synaptic dysfunction leading to cognitive impairments in hippocampal aging.

1.4 | Glia and $A_{2A}R$ dysregulation

Considering that any interference at the functional level of glial cells may create conditions favouring the development of degenerative processes, the key position of adenosinergic system in the control of glial function (Daré et al., 2007) has received increasing attention as a potential target in the modulation of neurodegenerative diseases, allowing to interfere at different components of the pathological condition, slowing down their progression (Fredholm et al., 2005).

1.4.1 | Microglia

Along the past years, growing evidence have generated new links between the brain and immune system, suggesting their intricate connection and significant crosstalk, both in the maintenance of homeostasis and in the progression of aging and neurodegenerative diseases (Lucin & Wyss-Coray, 2009).

Microglia, a cellular subset derived from myeloid precursors, are the gatekeepers of CNS immunology, establishing its first line of defence. Constituting approximately 10% of the total population of glial cells in the adult, their density varies considerably with anatomical region, ranging from a high of 12% in the basal ganglia to a low of 5% in the cortex of mice (Lawson et al., 1992). Considered to be the most susceptible sensors of brain pathology, microglial cells are endowed with numerous receptors capable of detecting physiological disturbances and continuously survey the entire brain parenchyma by constant extension and retraction of their thin and highly branched processes. Moreover, through a large number of signalling pathways, they are also able to communicate with neurons, astrocytes and immune cells, being key players of a functional neuroimmune interplay (Kettenmann et al., 2011). Therefore, through the integration of multifarious input signals, microglial cells display an extraordinary ability to respond rapidly and perform a broad range of functions in the modulation of CNS environment, from secretion of cytokines and chemokines which regulate the state of inflammation, to the release of mediators that control synaptic transmission, and phagocytosis of cells or cellular elements (Tambuyzer et al., 2009).

Following the detection of pathogens, brain lesion or nervous system dysfunction, microglia undergo a complex, multistage activation process that consists of a morphological transformation from a ramified to amoeboid appearance, in which these cells reduce the complexity of their shape and acquire characteristics resembling peripheral macrophages. Several steps and intermediate stages can be identified, including features of process withdrawal, transition or hyperramification, reflecting the high morphological plasticity of this cell subset and its functional adaption to its microenvironment (Kettenmann et al., 2011; Olah et al., 2011).

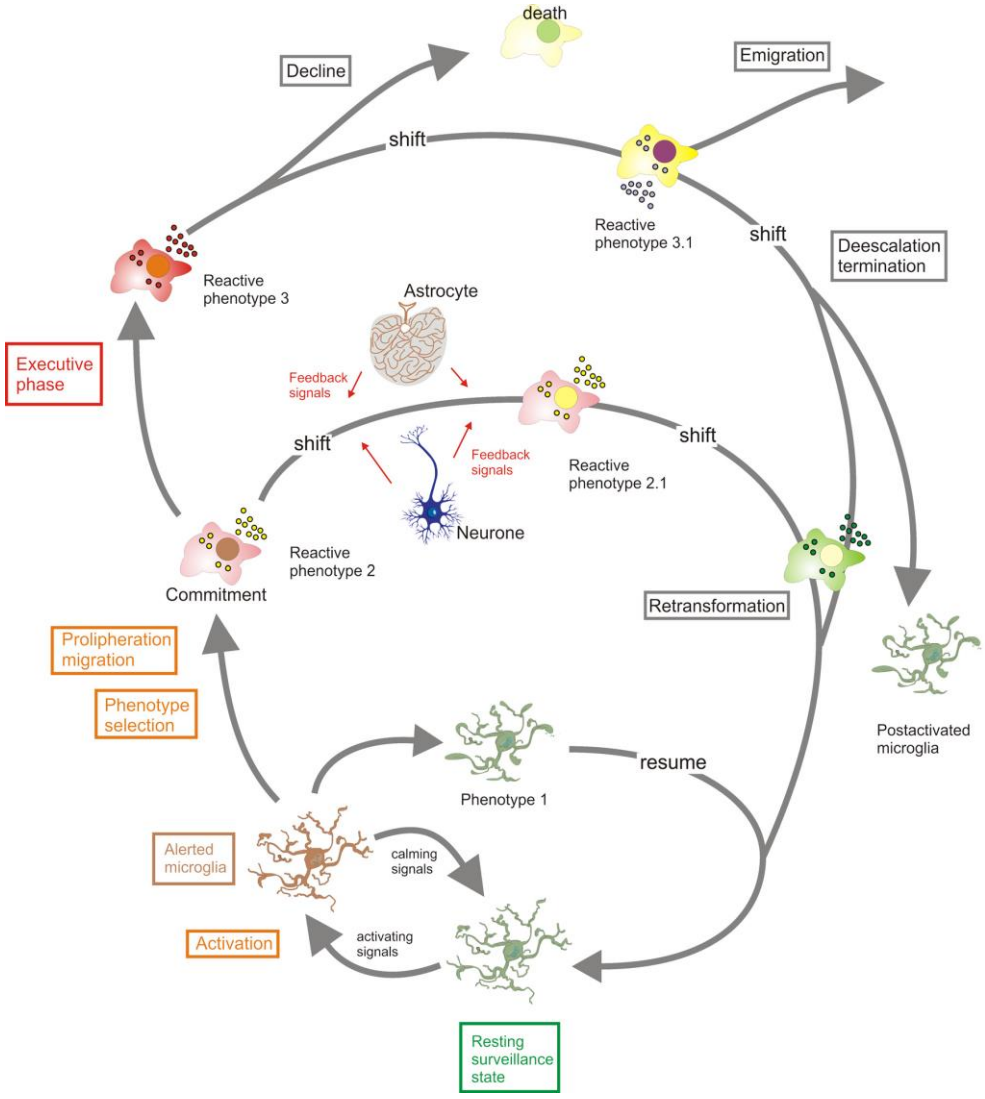

Figure 1.2 - **Schematic representation of microglial activation as a complex, multistage process**. Cells can commit to distinct reactive phenotypes depending on the challenging stimuli and situational context (from Kettenmann et al., 2011)

Depending on the interpretation of a given insult, microglia can acquire a “classically activated” M1 phenotype - characterized by the secretion of proinflammatory mediators such as Tumor Necrosis Factor α (TNFα) or IL-1β, Nitric Oxide (NO), and glutamate – or an “alternatively activated” M2 phenotype with the expression of anti-inflammatory factors - IL-4 and IL-13, for instance - which can enhance neuronal survival (Ji et al., 2013). Accordingly, M1 microglia have been associated with

neurotoxic and neurodegenerative processes, as it has been reported in cases of AD (Mandrekar-Colucci et al., 2012), Amyotrophic Lateral Sclerosis (Liao et al., 2012), Multiple Sclerosis (Gao & Tsirka, 2011), Stroke and Traumatic Brain Injury (Hu et al., 2012; Kumar et al., 2013), whereas a shift to an M2 phenotype has been correlated with neuroprotection, recovery and repair in various disease contexts (Mikita et al., 2011; Wu et al., 2012; Shechter & Schwartz, 2013).

Table 1.1: Cytokines produced upon microglial activation (adapted from Tambuyzer et al., 2009)

Cytokines	
IL-1α/β	IL-16
IL-3	IL-17
IL-4	IL-18
IL-5	IL-23
IL-6	IL-27
IL-8	TNF-α
IL-10	TGF-β
IL-12	IFN-γ
IL-13	GM-CSF
IL-15	M-CSF

Abbreviations: IL- Interleukin; TNF- Tumor Necrosis Factor; TGF – Transforming Growth Factor; GM-CSF – Granulocyte-Macrophage Colony-Stimulating Factor; M-CSF - Macrophage Colony-Stimulating Factor.

Due to the complexity of microglial cells and their high morphological and functional plasticity, histological approaches in conjunction with flow cytometry are critical to perform a full phenotypic characterization.

As a result of their myeloid lineage, the lack of specific microglial-only antigens has hampered microglial identification, since markers used for the detection of microglia are also present in macrophages. Consequently, microglial cells can be identified by a variety of cell surface-associated or intercellular/cytosolic molecules, concerning receptors, adhesion molecules and enzymes (Kettenmann et al., 2011; Hooper & Pocock, 2015), as resumed in **Table 1.2**.

Noteworthy, antibodies against Iba1 have proven most helpful in visualizing microglia with details of their processes (Kettenmann et al., 2011), while $CD45^{low}CD11b/c^{+}$ phenotype has been proven to describe ramified parenchymal microglia (Ford et al., 1995), which justifies the preferential use of these markers in the identification of this cellular subset. Nonetheless, the functional changes inherent to the activation process upregulate the expression level of many of these molecules, such as CD11b (Roy et al., 2006) and Iba1 (Ito et al., 2001), with reactive microglia expressing MHC class II antigens, CD40, CD54, CD68, CD80/86 and other surface molecules necessary for antigen presentation and phagocytosis (Kettenmann et al., 2011; Ford et al., 1995; Hooper & Pocock, 2015; Sedgwick et al., 1991).

Table 1.2: Principal microglial markers (Adapted from Kettenmann et al., 2011; Tambuyzer et al., 2009)

Molecular Structure/Antigen	Properties and Functional Relevance
CD11b/18 ($\alpha_M\beta_2$ integrin)	Complement receptor 3 (CR3)
CD11c (integrin αX)	Cell adhesion
CD16/32/64 (FcγRIII/II/I)	Immunoglobulin Receptors
CD34	Roles in adhesion, marker for precursor cells of myeloid origin
CD40	Tumor Necrosis Factor (TNF) Receptor
CD45 (Leucocyte Common Antigen)	Transmembrane protein tyrosine phosphatase
CD54 (Intracellular Adhesion Molecule 1)	Stabilization of cell-cell interactions
CD68	Phagocytosis
CD80/86 (B7.1/B7.2)	Antigen Presentation
CD200R	Myeloid cell inhibitory signalling Important for neuron-microglia communication
CX3CR1	Fractalkine (CX3CL1) receptor Control of microglial activity (neuron-microglia communication)
F4/80	Suggested role in immune tolerance
Iba1 (Ionized Calcium-binding adaptor molecule 1)	Suggested role in calcium homeostasis
iNOS (inducible NO synthase)	Enzymatic synthesis of NO from arginine during inflammation
MHC I/ II	Antigen presentation

Microglial activation is also highly influenced by neurons, through ‘on’ and ‘off’ signals, which are responsible for an inhibitory feedback in the absence of neuronal damage (Biber et al., 2007). This signalling system involve several ligands and receptors – CX3CL1-CX3CR1, CD200-CD200R, CD47-CD172a, for instance – that allow CNS to actively control local immune responses, modulating microglia number, activation and recruitment to sites of injury (Cardona et al., 2006; Olah et al., 2011).

Moreover, microglia are also considered to be active contributors in a paradigm of “quad-partite synapse” either through direct action on neurons or indirectly via astrocytes. Synaptic activity can alter microglial functioning in several aspects, including membrane potential, intracellular calcium, cytokine release and overall cellular motility, due to their ability to express receptors for and respond to neurotransmitters such as glutamate, GABA, acetylcholine, and purines, including adenosine and ATP (Schafer et al., 2013; Kettenmann et al., 2011; Pocock & Kettenmann, 2007). Conversely, in addition to their capacity to rapidly modulate their dynamics in response to neurotransmission, evidences also suggest an important role in the regulation of synaptic transmission (Ji et al., 2013; Schafer et al., 2013). Particularly in the hippocampus, several associations between soluble factors released by microglia and actions upon basal transmission and synaptic plasticity have been demonstrated, namely relating the secretion of Glycine and L-serine to the enhancement of LTP and NMDA receptor-mediated responses (Moriguchi et al., 2003; Hayashi et al., 2006), a link between

TNF-α and synaptic scalling (Stellwagen & Malenka, 2006) and a relation between ATP release and the modulation of basal glutamatergic transmission (Pascual et al., 2012). Lastly, besides synaptic plasticity, microglia also play dynamic roles at developing and mature synapses by the remodelling and maturation of synaptic circuits, being crucial to normal brain wiring and function (Schafer et al., 2013; Santiago et al., 2014). Therefore, this ability to shape neuronal environment according to the functional state of synapses through phagocytosis of synaptic elements, together with their role in the modulation of neurotransmission highlight the relevance of microglia as promotors of the homeostasis and long-term stability of neural networks.

The process of neuroinflammation is known to contribute to the exacerbation of neuronal damage. In fact, contexts of neurodegeneration are bolstered by dysregulation of microglial function, presenting features of abnormal synaptic transmission, aberrant synapse formation and/or elimination and abnormal phagocytosis as pathological hallmarks. Accordingly, increased levels of activated microglia have been correlated with most noxious brain conditions (Cunha, 2005) and degenerated brain regions in animal models and post-mortem examination of cases of AD and Parkinson's Disease (PD) (McGeer et al., 1987, 1988; Su et al., 2008). In agreement, the blockade of microglia-induced neuroinflammation has been proven to attenuate neurodegeneration (Santiago et al., 2014), which further supports their involvement in the evolution of the pathological process.

Consistent with the known ability of $A_{2A}R$ to control the activation of different inflammatory cell types, an increase in the expression of $A_{2A}R$ by microglial cells following their activation have been reported upon different brain insults (Canas et al., 2004; Yu et al., 2008). The hypothesis of $A_{2A}R$ modulation of microglia-induced neuroinflammation, controlling the genesis of the neuroinflammatory feedforward loop that leads to neurodegeneration, synaptic and cognitive impairments is supported by several studies in which $A_{2A}R$ blockade is sufficient to abrogate the Lipopolysaccharide (LPS)-induced microglial activation and consequent neuronal dysfunction (Rebola et al., 2011), reduce microinflammation in different pathological conditions (Laurent et al., 2014; Yu et al., 2008; Dai et al., 2010), improve microglia response to tissue damage and reduce cognitive impairments in AD and PD animal models (Gyoneva et al., 2014; Arendash et al., 2009; Ferreira et al., 2015). Therefore, therapeutic approaches of neuroinflammation modulation may represent a strategy for the attenuation of the neurological impairment underlying neurodegeneration, exploring the functional interplay between $A_{2A}R$ and microglial cells.

1.4.2 | Astrocytes

Astrocytes are the most abundant and heterogeneous cell type in the CNS, being responsible for the promotion of homeostasis through a wide range of essential complex functions (Sofroniew & Vinters, 2010). Occupying 25% to 50% of brain volume (Magistretti & Ransom, 2002), their star-shaped morphology provides structural support to the CNS, forming the infrastructure on which other cells are anchored. Astrocytic multiple fine processes intertwine with neurons, ensheath dendrites and synapses and surround brain capillaries, integrating neuro and vascular elements within an individual astroglial territorial domain, thereby dividing brain parenchyma into independent neurovascular units (Kettenmann & Verkhratsky, 2011).

In addition to their structural role, astrocytes support and modulate synaptic transmission by means of numerous coordinated mechanisms. Through the expression of functional neurotransmitter receptors (glutamate, ATP, GABA, acetylcholine or endocanabinoids) (Oberheim et al., 2012), information shared inside and outside synapses is continuously sensed and elicits astrocytic calcium signalling, promoting the release of neuro and vasoactive substances - such as glutamate, D-serine, ATP, GABA, TNF-α, prostaglandins and peptides - which lead to feedback regulation of neuronal activity, synaptic strength, blood flow and metabolism, in a process known as gliotransmission (Stehberg et al., 2012). Moreover, astrocytic network is also crucial in spatial buffering of K+ and regulation of ion concentrations, as well as in neurotransmitter homeostasis, by ensuring glutamate-glutamine turnover, contributing to an overall neuronal protection against excitotoxicity (Magistretti & Ransom, 2002; Pekny et al., 2016).

Furthermore, reactive astrocytes are critical for tissue repair and function maintenance in the CNS. Following brain insults, astrocytes undergo a multicomponent activation process designated astrogliosis which consists on a continuum of complex changes that occur in a context-dependent manner, leading to profound changes in astrocytic biochemistry and physiology, by activation of pathways involved in inflammation, metabolism, cytoarchitecture and microenvironmental regulation. Thus, reactive astrocytes acquire the ability to release diverse molecular signals, both anti- and pro-inflammatory factors, capable of affecting the activity of different types of surrounding cells, in an attempt to increase neuroprotection (Pekny et al., 2016; Sofroniew & Vinters, 2010) (**Figure 1.3**).

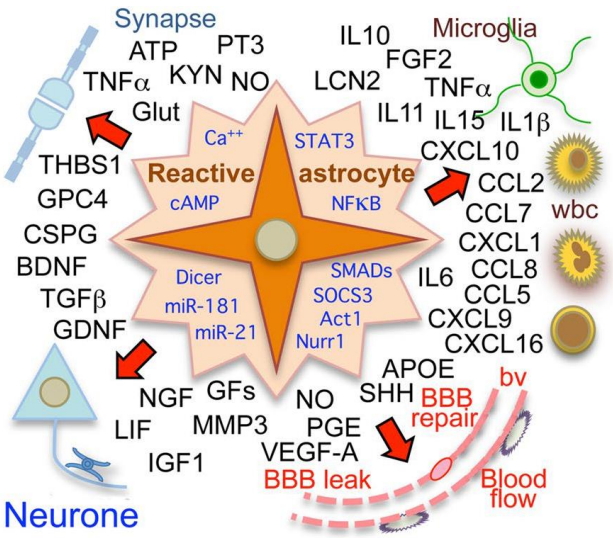

Figure 1.3: Schematic representation of molecular signals sent by reactive astrocytes. Reactive astrocytes establish complex signalling interactions with different cell types through the release of numerous growth factors, neurotransmitters, cytokines and chemokines (from Pekny et al., 2016)

Although reactive astrogliosis is protective in acute responses, limiting the extent of neurodegeneration, if it persists, long-lasting scar formation might be promoted, along with a shift towards a pro-inflammatory and potentially cytotoxic phenotype, resulting in permanent rearrangement and insult of brain parenchyma (Pekny et al., 2016; Sofroniew & Vinters, 2010).

Actually, dysfunction or maladaptative responses of astroglia are known features of neurodegenerative processes, contributing and exacerbating the progression of several diseases. At a neuropathological level, astrocyte changes are highly variable and disease specific, concerning phenotypes of exarbated astrogliosis response, pathological remodeling and atrophy with loss of function, which can be simultaneously present or emerge sequentially with disease progression (Pekny et al., 2016; Maragakis & Rothstein, 2006) (**Figure 1.4**)

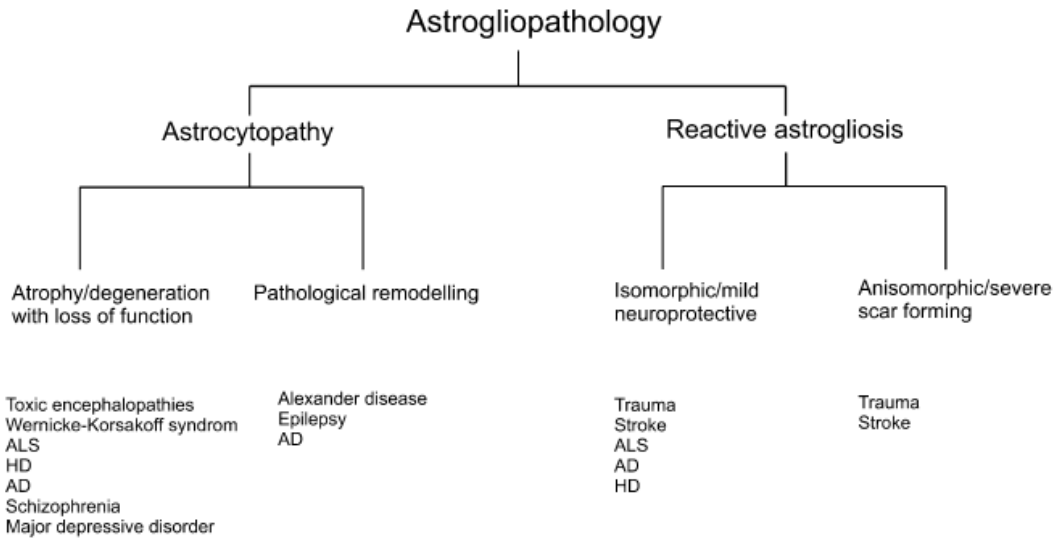

Figure 1.4 - Schematic representation of pathological changes in astroglia. Astroglial component of neuropathology is highly variable and is often disease specific (from Pekny et al., 2016)

The complex process of astrogliosis can be induced and directly modulated by a broad range of extracellular molecules, from purines, neurotransmitters and steroid hormones to growth factors, cytokines, serum proteins or neurodegeneration-associated molecules (Pekny et al., 2016). In fact, adenosine and $A_{2A}R$ can modulate astrocytic function both through the control of astrogliosis and consequent release of different substances that influence synaptic activity, or by an indirect fine-tuning of the action of other receptor systems in astrocytes (Daré et al., 2007). As $A_{2A}R$ activation can inhibit EAAT2-mediated astrocytic glutamate uptake and enhance glutamate release (Cunha, 2005), the detrimental effects of high levels of adenosine deriving from prolonged or exaggerated exposure to noxious brain conditions are also result of an inflicted dysregulation of astroglial function.

2 | AIMS

Noxious brain conditions such as hypoxia, ischemia, epilepsy, stress or aging are known to induce an inbalance of adenosinergic system, characterized by a long term robust upregulation of $A_{2A}R$ in cortical and hippocampal regions, which leads to excitotoxicity, dendritic retraction and memory and synaptic plasticity impairment. Although the mechanism involved in this $A_{2A}R$ upsurge and which exactly are the neurotransmitters or neuronal pool directly affected are yet unknown, different studies have been linking this changes concerning adenosine receptor system upon brain insults with those found in aged animals, raising an early-aging hypothesis behind neurodegeneration.

Having as hypothesis that $A_{2A}R$ dysregulation in the genesis of synaptic dysfunction and cognitive impairments in hippocampal aging derives from glutamatergic neurons, transgenic rats with a postnatal $A_{2A}R$ overexpression conditional to the glutamatergic forebrain neurons (Tg(CaMKII-h$A_{2A}R$), have been generated. Since this animal model displays age-like alterations in hippocampal function, with cognitive, synaptic and molecular impairments, it constitutes an unprecedented model to detail $A_{2A}R$ dysregulation in the hippocampus.

Therefore, this study aimed **to evaluate the contribution of different cellular subsets to the pathological phenomena associated with A_{2A} receptors dysregulation in the hippocampus**.

As the modulatory potential of adenosine is also extended to the control of glial cell function, **it was assessed if this neuronal-specific overexpression of $A_{2A}R$ drives alterations in the reactivity of astrocytes and microglia**, exploring the contribution of these cells to the hippocampal dysfunction. Moreover, it was also aimed to assess impacts on hippocampal circuitry, **analyzing secondary effects of a glutamatergic-specific $A_{2A}R$ overexpression.**

Clarifying the involvement of different cellular subsets in the $A_{2A}R$ dysregulation underlying synaptic and cognitive dysfunction will be helpful to improve knowledge of neuropathology, including aging and neurodegeneration.

3 | METHODS

3.1 | Animals

Animal procedures were performed within the rules of the Portuguese official veterinary department, which complies with European Directive 2010/63/EC and the Portuguese law transposing this Directive (DL 113/2013), and approved by the Instituto de Medicina Molecular Internal Committee and the Portuguese Animal Ethics Committee (Direcção Geral de Veterinária). Environmental conditions were kept constant: food and water *ad libitum*, 21±0.5°C, 60±10% relative humidity, 12 h light/dark cycles.

A model of transgenic rats that overexpress $A_{2A}R$ - Tg(CaMKII-h$A_{2A}R$) - was used, as described in Coelho et al. (2014). These were generated by microinjection of a linearized DNA construct **(Supplementary Figure 7.1)** into male pronucleus of Sprague-Dawley rat zygotes, consisting on a full-length human A_{2A} cDNA cloned into an expression vector with the 8.5kb mouse CaMKIIα promoter and a polyadenylation cassete of bovine growth hormone. Littermate WT animals were used as controls.

3.2 | Genotyping

Transgenic rats were identified by Polymerase Chain Reaction (PCR) (30 cycles, 58ºC annealing temperature) of their genomic DNA isolated from ear biopsies by the use of transgene-specific primers: CaMKII-h$A_{2A}R$ and rat β-actin (Invitrogen, **Table 3.1**)

Table 3.1 - Primers used for genotyping of transgenic animals

Primer	Target Gene	Organism	Forward Primer	Reverse Primer	Amplicon Size
Act-B	β-actin	Rat	AGCCATGTACGTAGCCAT	CTCTCAGCTGTGGTGGTGAA	228 bp
CaMKII-h$A_{2A}R$	Calcium calmodulin-dependent Protein Kinase II promoter and human Adenosine A_{2A} Receptor	Transgene	GACTAAGTTTGTTCGCATCCC	GTGACACCACAAAGTAGTTGG	450 bp

3.3 | Hippocampal Cell Dissociation

Based on Kay & Wong (1986), animals with about 8 weeks old were decapitated under deep anesthesia by Isofluorane, hippocampi were removed and sliced at 650µm thickness with a McIlwain tissue chopper. CA1 and CA3 regions of 6 slices per hippocampus were dissected and incubated at

32ºC for 5 minutes in an oxygen saturated dissociation solution (120mM NaCl, 5mM KCl, 1mM $CaCl_2$, 1mM $MgCl_2$, 25mM Glucose and 20mM PIPES) with 0.2mg/ml of Proteinase K, followed by a 30 minutes incubation at 32ºC with 1mg/ml Trypsin diluted in oxygen saturated dissociation solution.

After chemical dissociation, slices were transferred to an oxygen saturated enzyme-free dissociation solution, briefly washed, and each slice was mechanically dissociated in 1ml of Dulbecco's Modified Eagle's Medium (DMEM) (Gibco – Life Technologies) by gentle trituration, using 2 fire polished Pasteur pipettes (1 and 0.2 mm bore). Immediately after trituration, 500µl of supernatant was plated per well on poly-D-lysine-coated coverslips in 24-well plates, and incubated for 30 minutes to promote cell decantation. After removing medium from wells, immunocytochemistry protocol was performed.

3.4 | Primary Neuronal Cultures

Primary rat neuronal cultures were obtained from 18 days rat embryos, according to Pedersen et al (2002). Briefly, a pregnant rat, previously genotyped as Transgenic (Tg(CaMKII-hA_{2A}R)) was decapitated under deep anesthesia with Isofluorane. The embryos were collected in Hanks' Balanced Salt Solution (HBSS) (Corning) and rapidly decapitated. Meninges were removed, whole cortices (hippocampi and attached cortex) dissociated and incubated for 15 minutes in HBSS with 0.025% trypsin. Cells were washed once with HBSS with 30% Fetal Bovine Serum (FBS), centrifuged three times, re-suspended in Neurobasal Medium (Gibco – Life Technologies) supplemented with 2% B-27 supplement, 25 µM Glutamate, 0.5 mM glutamine, and 2 U/ml Penicillin/Streptomycin, gently dissociated and filtered through a 70µm strainer (VWR).

After counting, cells were plated on poly-D-lysine-coated coverslips in 24-well plates at density of $8x10^4$ cells/well. Neurons were grown at 37°C in a 5% CO_2 humidified atmosphere in the previously described supplemented Neurobasal medium, in the absence of any positive selection for neurons. Medium was not replaced and cultures were used at day 9 and 14.

3.5 | Immunocytochemistry

Cells from either hippocampal dissociation or primary neuronal cultures were fixed for 10 minutes with 4% Paraformaldehyde (PFA) diluted in Phosphate Buffer Saline (PBS) (Alpha Aesar). After washing thrice with PBS, cells were permeabilized for 10 minutes with 0.05% Triton-X in PBS, blocked for 30 minutes with 10% FBS in PBS and incubated overnight at 4°C with primary antibodies diluted in PBS with 0.05% Tween-20 and 4% FBS **(Table 3.2)**.

After washing three times with PBS with 0.05% Tween-20, cells were incubated for 1 hour with secondary antibodies diluted in PBS with 0.05% Tween-20 and 4% FBS **(Table 3.2)**. In order to label cell nucleus, after washing 30 minutes with PBS with 0.05% Tween-20, coverslips were incubated

for 5 minutes with Hoechst (Hoechst 33342, Thermo Scientific; 12µg/ml final concentration) and washed for 30 minutes with PBS 0.05% Tween-20. After a final washing step with PBS, coverslips were mounted with Dako Fluorescent Mounting Medium (Dako) and let to dry for 24h at room temperature, protected from light exposure.

Cells were observed either with a Zeiss Axiovert 200M Fluorescence Microscope or a Zeiss LSM 710 Confocal Microscope.

Table 3.2 - Primary and secondary antibodies and related conditions used in the Immunocytochemistry experiments. All antibodies were diluted in PBS with 0.05% Tween-20 and 4% FBS

Protein	Primary Antibody	Host	Dilution	Secondary Antibody (from Life Technologies)	Dilution
$A_{2A}R$	Santa Cruz Biotechnologies (SC-7502)	Goat	1:100	Alexa Fluor 633 donkey anti-goat	1:400
$A_{2A}R$	Millipore (clone 7F6-G5-A2)	Mouse	1:100	Alexa Fluor 568 donkey anti-mouse Alexa Fluor 488 goat anti-mouse IgG2a (γ2a)	1:400
FLAG	Sigma-Aldrich (F7425)	Rabbit	1:200	Alexa Fluor 488 donkey anti-rabbit	1:400
MAP-2	Millipore (05717)	Rabbit	1:200		
SYP	Sigma-Aldrich (S5768)	Mouse	1:250	Alexa Fluor 568 donkey anti-mouse	1:400
PSD-95	Cell Signalling (D27E11)	Rabbit	1:500	Alexa Fluor 488 donkey anti-rabbit	

Abbreviations: $A_{2A}R$ – Adenosine A_{2A} Receptor; MAP-2 - Microtubule-associated protein 2; SYP – Synaptophysin; PSD-95 - Postsynaptic Density Protein 95

3.6 | Brain Perfusion

Animals with 12 to 14 weeks old were deeply anaesthetized with an Intraperitonial Injection of a mixture containing Ketamine and Xylazine (120mg/KgBW Ketamine + 16mg/KgBW Xylazine) and transcardially perfused via the ascending aorta. A lateral incision was made below the sternum and xiphoid process was held with forceps. The diaphragm was cut and an incision was made parallel to the sternum to expose the thoracic cavity. A needle was inserted into left ventricle, and the right atrium perfurated to initiate perfusion. Animals were perfused with 200ml of a 0.9% NaCl solution and subsequently perfused with 500ml of 4% PFA diluted in PBS. After perfusion, animals were decapitated, brains were removed and cryopreserved in a 15% sucrose in PBS solution overnight at 4ºC, followed by 30% sucrose in PBS solution during 48h at 4ºC.

3.7 | Gelatin Embedding

After cryopreservation in 15 and 30% sucrose, brains were equilibrated with a 15% sucrose/7.5% gelatin in PBS solution for 1h at 37ºC, embeded in the same solution and left to solidify overnight at 4ºC. The included tissue was cut into blocks and slowly frozen to -70ºC by submerging in isopentane cooled with liquid nitrogen. The blocks were kept at -80ºC until use.

3.8 | Immunohistochemistry

Coronal cryostat sections of 12µm - starting at approximately -3.14mm from Bregma - were collected with a CM3050S Leica cryostat and mounted in Superfrost Slides (Thermo Scientific).

For immunohistochemistry, the slides were incubated in PBS for 10 minutes at 37ºC followed by a 20 minutes incubation with 0.1M glycine in PBS. The slices were then permeabilized and blocked with a solution of TBST-T 0.2% (Tris Buffer Saline with 0.2% Tween-20 solution, 200nM Tris, 1.5 M NaCl) containing 10% FBS and 1% BSA (Bovine Serum Albumin) for 1 hour. Incubations with primary antibodies (**Table 3.3**) were performed for 48h at 4ºC and slices were washed for 30 minutes in TBS-T 0.1% (Tris Buffer Saline with 0.1% Tween-20 solution, 200nM Tris, 1.5 M NaCl) before being incubated overnight at 4ºC with secondary antibodies (**Table 3.3**). After a 30 minutes washing with TBS-T 0.1%, slices were incubated for 10 minutes with Hoechst (Hoechst 33342, Thermo Scientific; 12µg/ml final concentration) and washed for 15 minutes with PBS. Lastly, slices were mounted in Dako Fluorescent Mounting Medium (Dako) and left to dry for 24h at room temperature protected from light exposure.

Table 3.3 Primary and secondary antibodies and related conditions used in the Immunohistochemistry experiments. All antibodies were diluted in TBS-T 0.1% with 4% FBS.

Protein	Primary Antibody	Host	Dilution	Secondary Antibody	Dilution
$A_{2A}R$	Santa Cruz Biotechnologies (SC-7502)	Goat	1:100	Abcam (Donkey anti-goat cy3)	1:400
FLAG	Sigma-Aldrich (F7425)	Rabbit	1:200		
Iba1	Abcam (ab5076)	Goat	1:200	Life Technologies (Alexa Fluor 633 donkey anti-goat, Alexa Fluor 568 donkey anti-mouse Alexa Fluor 488 donkey anti-rabbit 488)	1:400
GFAP	Millipore (MAB360)	Mouse	1:250		
SYP	Sigma-Aldrich (S5768)	Mouse	1:250		
PSD-95	Cell Signalling (D27E11)	Rabbit	1:400		

Abbreviations: $A_{2A}R$ – Adenosine A_{2A} Receptor; Iba1 - Ionized Calcium-Binding Adapter Molecule 1; GFAP - Glial Fibrillary Acidic Protein; SYP – Synaptophysin; PSD-95 - Postsynaptic Density Protein 95

3.9 | DNA extraction and sequencing

DNA was extracted using NucleoSpin Gel and PCR Clean-Up Kit (Macherey-Nagel). Briefly, after electrophoresis of PCR products of genotyping procedure, 2 bands of agarose gel containing the 450 bp fragment amplified using CaMKII-hA_{2A}R specific primers (see Table 3.1) were excised.

After agarose was dissolved, samples were loaded into a column and centrifuged twice for 30 seconds at 11000 xg, in order to bind DNA to a silica membrane and to promote its washing. Then, the membrane was dried and DNA eluted. Lastly, DNA was analyzed with Nanodrop 2000 Spectrophotometer (Thermo Scientific) and sent for sequencing (GATC Biotech) using CaMKII-hA_{2A}R specific primers at a 5μM concentration.

3.10 | Sample preparation for Western Blotting

Frozen hippocampal tissue was placed in 400μl of RIPA (Radio-Immunoprecipitation-Assay) buffer (50mM Tris, 1mM EDTA, 150mM NaCl, 0.1% SDS, 1% NP-40, pH 8) and homogenized by sonication. Protein was quantified using the BioRad DC Protein Assay Kit, based on Lowry (1951), due to the high levels of detergents in the sample.

After protein quantification, the appropriate volume of each sample was diluted in four volumes of water and one volume of sample buffer (350 mM Tris pH 6.8, 30% glycerol, 10% SDS, 600 mM DTT and 0.012% Bromophenol blue). The samples were denatured at 95°C for 5 minutes.

3.11 | Western Blotting

Based on the protocol of Towbin et al. (1979), samples and molecular weight markers were separated by SDS-PAGE electrophoresis in denaturing conditions, using 5% stacking gel and either a 10% or 15% resolving gel, and electro-transferred to PVDF membranes (Millipore). Membranes were blocked with 3% BSA in TBS-T 0.1% for 1 hour and incubated with primary antibody (diluted in TBS-T with 3% BSA) overnight at 4°C in a roller. After washing with TBS-T for 30 minutes, the membranes were incubated with horseradish peroxidase (HRP, EC 1.11.1.7) conjugated secondary antibody in 5% non-fat dry milk for 1 hour at room temperature (primary and secondary antibody dilutions are in **Table 3.4**). After 30 minutes of washing with TBS-T, chemoluminescent detection was performed with ECL Western Blotting Detection Reagent (GE Healthcare) using X-Ray films (Fujifilm) developed in Curix 60 Processor (AGFA). Optical density was determined with ImageJ software and normalized to the respective GAPDH band density.

Table 3.4 - Primary and secondary antibodies and related conditions used in the Western Blotting experiments for individual proteins. All primary antibodies were diluted in TBS-T 0.1% with 3% BSA and secondary antibodies in 5% non-fat dry milk diluted in TBS-T 0.1%

Protein	Protein Loading (µg)	Resolving Gel (%)	Primary Antibody	Host	Dilution	Secondary Antibody	Dilution
FLAG	30	10	Sigma-Aldrich (F7425)	Rabbit	1:320	Santa Cruz Biotechnologies (Donkey anti-goat, Goat anti-mouse Goat anti-rabbit)	1:10000
Iba1	30	15	Abcam (ab5076)	Goat	1:500		
PSD-95	30	10	Cell Signalling (D27E11)	Rabbit	1:1000		
GFAP	30	10	Millipore (MAB360)	Mouse	1:1000		
SNAP-25	30	15	Sigma-Aldrich (S9684)	Rabbit	1:10000		
GAPDH	-	-	Life Technologies (6C5)	Mouse	1:1000		

Abbreviations: Iba1 - Ionized Calcium-Binding Adapter Molecule 1; PSD-95 - Postsynaptic Density Protein 95; GFAP - Glial Fibrillary Acidic Protein; SNAP-25 - Synaptosomal-Associated Protein 25; GAPDH - Glyceraldehyde 3-Phosphate Dehydrogenase

3.12 | Analysis of Neuronal Cell Number

Per animal, four fields of CA1 pyramidal cell layer were randomly selected of 12µm hippocampal slices and acquired at 40x magnification using a Zeiss Cell Observer Widefield microscope. Cells labeled with Hoechst were counted using Cell Counter Plugin of ImageJ software.

3.13 | Morphological analysis of microglial cells

Confocal Z-stacks of 12µm slices stained with Iba1 were taken at 20x magnification, using a Zeiss LSM 710 Confocal Microscope.

Based on Almolda et al. (2015), a morphometric analysis of Iba1 labeled microglia was performed. For each animal, a total of 60 representative microglial cells from CA1 area were chosen from a minimum of 10 different z-stack images. Using ImageJ software, maximum intensity projection images were generated and individual cells were isolated by the tracing of their perimeter with Polygon Selection tool. Different parameters including the fitted ellipse were recorded for each cell.

3.14 | Flow Cytometry

After deep anesthesia with Isofluorane, rats were perfused with approximately 200ml of PBS via the left ventricle of the heart to exclude circulating and nonadherent erythrocytes and leukocytes from the brain. Brains were removed, hippocampi were dissected on ice-cold Krebs Buffer (124mM NaCl, 3mM KCl, 1.25mM Na_2HPO_4, 26mM $NaHCO_3$, 1mM $MgSO_4$, 2mM $CaCl_2$, 10mM glucose) and minced with a razor blade in ice-cold GKN/BSA Buffer (GKN: 8g/l NaCl, 0.4g/l KCl, 3.6g/l $Na_2HPO_4.12H_2O$, 0.8g/l NaH_2PO_4, 2g/l D-(+)-glucose, 0.3% BSA, pH 7.4, 4ºC).

Two experimental conditions were performed. Firstly, according to Doorn et al. (2015), identical regions of 2 animals were pooled per experiment to increase microglial yield and tissue was gently dissociated in GKN/BSA Buffer, mashed through a 70µm pore size strainer (VWR) to reach a single cell suspension and centrifuged for 10 minutes at 300g at 4ºC. The supernatant was discarded and the remaining cell pellet was resuspended in 1ml of 50% Percoll diluted in GKN/BSA buffer, after which an additional 7ml 50% Percoll was added. Then, 4ml of 75% Percoll was gently under layered and subsequently 3ml GKN/BSA buffer was layered on top of the 50% Percoll layer. The Percoll gradient was centrifuged at 1300 xg, for 30min at 4ºC, with minimum acceleration and brakes off. After the removal of the top layer - composed of thick, viscous myelin – the interphase between the 50 and 75% Percoll was carefully removed using a Pasteur pipette, washed with GKN/BSA buffer and cells were resuspended in PBS buffer. 500µl aliquots of cell suspension were prepared and incubated for 30 minutes with FITC-conjugated anti-integrin αM/CD11b (OX42) antibody (Santa Cruz Biotechnologies, sc-53086, final dilution 1:200) and PE-conjugated anti-CD45 (OX30) antibody (Santa Cruz Biotechnologies, sc-53047, final dilution 1:200) at room temperature, in a rocker. Lastly, cells were rinsed in PBS, pelleted at 1200rpm for 5 minutes at 4ºC and ressuspended in 300µl PBS.

In the second experimental condition, the previous protocol was maintained with the exception of Percoll gradient, in order to obtain non-purified samples.

Data acquision was performed on a BDAccuri C6 Flow Cytometer (BD Biosciences) and analyzed using FlowJo software.

3.15 | GFAP DAB Immunohistochemistry

Coronal cryostat sections of 40µm - starting at approximately -3.14mm from Bregma - were collected with a CM3050S Leica cryostat and mounted in Superfrost Slides (Thermo Scientific) with intervals of 160µm, in order to obtain a set of non-contiguous serial sections spanning dorsal hippocampus.

Gelatin was removed from slices by incubation with PBS for 10 minutes at 37ºC. Staining was preformed using the EnVision+ System-HRP (DAB) from Dako. After washing 1 hour with Wash Buffer at room temperature, peroxidase was blocked with 3% H_2O_2 in methanol for 30 minutes.

Following washing 15 minutes with Wash Buffer, slices were blocked with Protein-Block for 40 minutes and incubated with Rabbit anti-GFAP polyclonal antibody (Dako) at a 1:500 dilution, for 2 hours at room temperature. After washing 15 minutes with Wash Buffer, slices were incubated with Anti-Rabbit antibody conjugated with HRP (Dako) for 1 hour at room temperature, and washed for 15 minutes washing with Wash Buffer. Slices were then stained with 3,3'-Diaminobenzidine (DAB) for 2 minutes and rinsed in distilled H_2O (dH_2O). Lastly, slices were dehydrated using a graded series of Ethanol (70%, 96%, 100%), cleared in Xylene and mounted.

3.16 | Morphological analysis of astroglial cells

Based on Morel et al. (2015), per animal, a set of three non-contiguous 40µm coronal cryostat sections was processed by GFAP DAB Immunohistochemistry and scanned with a NanoZoomer SQ slide scanner (Hamamatsu) under 20x magnification. In each set, a total of 90 representative GFAP+ cells of CA1 area were randomly chosen and analyzed using Sholl Analysis Plugin v1.0 of ImageJ software. This technique consists of individualizing cells by precise drawing and superimposing a grid with concentric rings distributed at equal distances centered on cell body. The number of process intersections per shell was then computed in order to evaluate length and complexity of astroglial branching.

3.17 | Statistics

GraphPad Prism 5 software was used for statistical analysis. The values presented are mean ±SEM of n experiments. To test the significance of differences between WT and Tg(CamKII-hA_{2A}R), unpaired Student's t-test was used. In the morphological analysis of astroglial cells, a two way ANOVA followed by a Bonferroni's Multiple Comparison post hoc test was used. Values of $P<0.05$ were considered to be statistically significant.

4.1 | Localization and secondary effects of $A_{2A}R$ overexpression

Previous results from our group have characterized the molecular features of the CaMKII-h$A_{2A}R$ transgenic model (**Supplementary Figure 7.5**), confirming that these animals overexpress $A_{2A}R$ mostly in the hippocampus, in the pre-synaptic region and from 2 weeks-old onwards. In sequence with this preliminary data, the current project had the purpose to investigate the localization of $A_{2A}R$ in Tg(CaMKII-h$A_{2A}R$) rat model, as well as the consequences of this upsurge in the pattern of expression of $A_{2A}R$ in different cellular subsets.

In order to do so, several approaches were possible, with advantages and disadvantages that were considered in the experimental strategy. Immunohistochemistry was the first method to be chosen, due to the advantage of preserving the structure of hippocampal tissue.

$A_{2A}R$ signal consisted of a puncta-like staining around cell body of neurons in both conditions **(Figure 4.1)**, not allowing to infer a viable conclusion, as the antibody used is not specific to the human subtype of $A_{2A}R$.

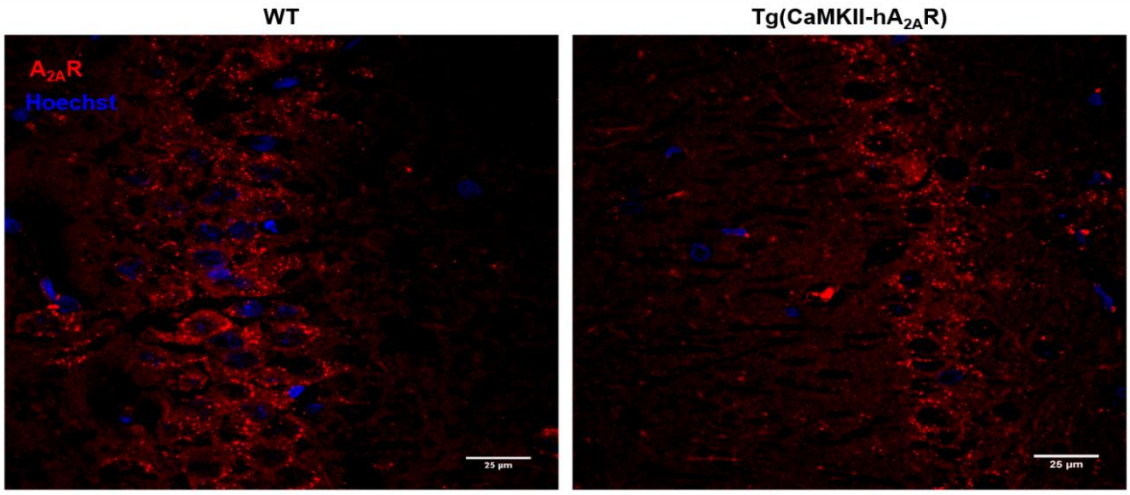

Figure 4.1 - $A_{2A}R$ staining by immunohistochemistry. Fluorescence immunohistochemistry images from CA1 area of 12µm rat hippocampal sections at 40x magnification. Neuronal nuclei are stained with Hoechst (blue) and $A_{2A}R$ are identified by red fluorescence using goat anti-human $A_{2A}R$ antibody (Santa Cruz Biotechnologies). Scale Bar:25µm.

With the intention of bypassing the difficulties inherent to $A_{2A}R$ antibodies, we tried to use the FLAG-tag included in the construct that generated Tg(CaMKII-h$A_{2A}R$) rats (**Supplementary Figure 7.1**) as a mean to locate transgenic $A_{2A}R$ receptor expression. Firstly, we extracted DNA from transgenic animals and sequenced the 450bp amplicon in order to assess if the FLAG-tag was successfully inserted in the transgene and correctly in fusion with the $A_{2A}R$ protein. Nonetheless, even though we confirmed that there is a FLAG epitope inserted in frame between 6 and 7th aminoacids of the N-terminal of the transgenic human $A_{2A}R$ protein (**Supplementary Figure 7.2**), anti-FLAG antibody

also failed to detect $A_{2A}R$ overexpression by Immunohistochemistry and Western Blotting (**Supplementary Figures 7.3 and 7.4**).

Considering that immunohistochemistry has the constraint of decreased epitope accessibility, primary neuronal cultures seemed a good alternative to promote antibody staining by enhancing epitope exposure. Thus, mouse anti-$A_{2A}R$ antibody (Millipore), goat anti-human $A_{2A}R$ antibody (Santa Cruz Biotechnologies) and rabbit anti-FLAG antibody (Sigma-Aldrich) were tested by Immunocytochemistry. The results obtained did not allow us to localize $A_{2A}R$ overexpression. However, it is difficult to recreate this model in primary neuronal cultures, since the overexpression of $A_{2A}R$ in transgenic animals is only post-natal (2 weeks-old onwards) and the progeny of heterozygous animals can lead to cultures with mixed genotypes, which can explain the lack of results.

Alternatively, we attempted to label $A_{2A}R$ in fully differentiated cells isolated from hippocampus of adult animals through enzymatic and mechanical dissociation. Nevertheless, this method did not allow us to detect any specific A_{2A} labelling, possibly reflecting an irreversible alteration of membrane channels by trypsin digestion, or a consequence of the loss of distal dentritic processes.

Lastly, in collaboration with Neuropathology Department of Hospital de Santa Maria, $A_{2A}R$ staining was performed using mouse anti-A_{2A} antibody (Millipore; clone 7F6-G5-A2) and HRP DAB detection and amplification systems, which enabled the detection of the human $A_{2A}R$ overexpression in CA3 axonal projections and in the neuropil of DG and CA1 areas of Tg(CaMKII-h$A_{2A}R$) animals **(Figure 4.2).**

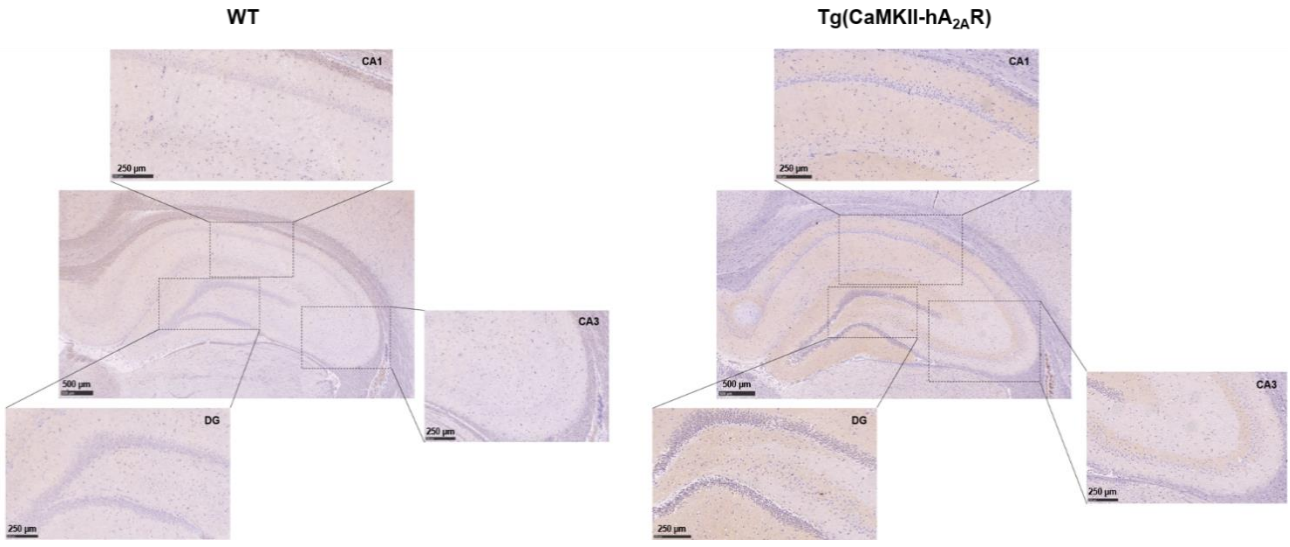

Figure 4.2 - Distribution of human $A_{2A}R$ overexpression in Tg(CaMKII-h$A_{2A}R$) rats. Staining was present in hippocampal and striatal areas of Tg(CaMKII-h$A_{2A}R$) animals but not WT littermates. Within the hippocampus, positive labelling can be observed in CA3 axonal projections and strong staining is also observed in the neuropil of DG and CA1 areas. Immunohistochemistry: brain tissue was fixed in formalin, processed, embedded and sectioned in paraffin. Coronal sections across the span of the brain were stained using a mouse anti-A_{2A} antibody (Millipore; clone 7F6-G5-A2) and

revealed using HRP-DAB detection and amplification systems. Images were acquired with NanoZoomer SQ slide scanner (Hamamatsu) under 20x magnification. (Staining performed by Dr. Pedro Pereira, Neuropathology Hospital Santa Maria, Lisbon).

4.2 | $A_{2A}R$ overexpression and neuronal loss

In order to assess if $A_{2A}R$ overexpression in forebrain neurons was correlated with synaptic loss, the number of neuronal cells in pyramidal layer of CA1 area and the levels of markers of synaptic density in the hippocampus were evaluated in CaMKII-h$A_{2A}R$ transgenic model.

4.2.1 | Neuronal cell counts in CA1 area

No significant differences were found in neuronal cell number of CA1 pyramidal layer in four randomly selected 40x fields of Tg(CaMKII-h$A_{2A}R$) (n=3) and WT littermates (n=2) (P>0.05) **(Figure 4.3)**.

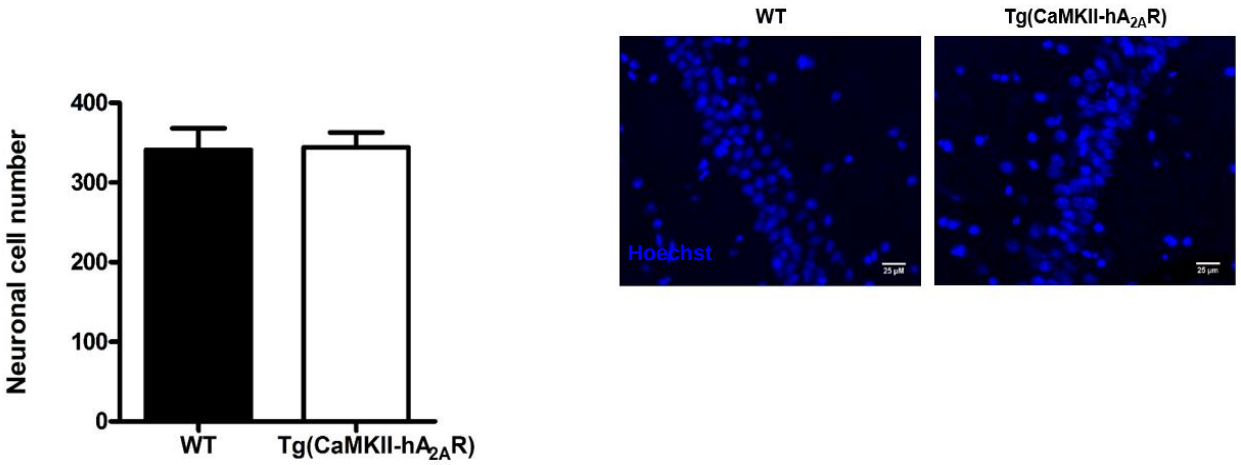

Figure 4.3 - Neuronal cell number in the CA1 area of hippocampus. Four fields of 40x magnification were randomly selected and analyzed per each WT (black) (n=2) or Tg(CaMKII-h$A_{2A}R$) (white) (n=3) animals. Results are presented as the mean ± SEM. At the right, representative images of neuronal nuclei stained with Hoechst are presented. Scale Bar: 25µm.

4.2.2 | Levels of markers of synaptic density

Synaptosomal-associated protein 25 (SNAP-25), a component of the SNARE complex, is a presynaptic plasma membrane protein involved in regulation of neurotransmitter release (Hodel, 1998). The levels of SNAP-25 were quantified by Western Blotting to assess presynaptic density.

Results revealed no significant changes in protein levels of SNAP-25 in Tg(CaMKII-hA_{2A}R) (n=7) compared to WT littermates (n=7) (P>0.05) **(Figure 4.4)**.

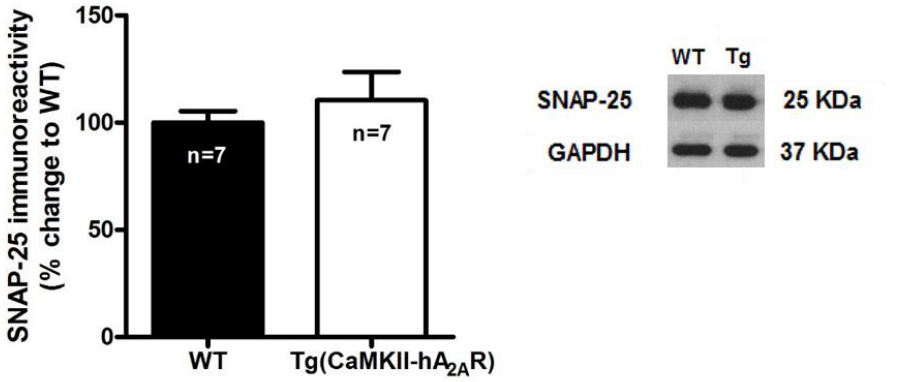

Figure 4.4 - SNAP-25 levels in the rat hippocampus. Immunoreactivity of SNAP-25 was measured in whole tissue homogenates either for WT (black) or Tg(CaMKII-hA_{2A}R) (white) animals. Specific immunoreactivity was normalized to that of GAPDH. Results are the mean ± SEM of seven experiments. At the right, a representative image of the Western Blot is presented.

Postsynaptic density protein 95 (PSD-95) is a membrane associated guanylate kinase scaffolding protein located in postsynaptic densities (Stathakis et al., 1997). The levels of PSD-95 were quantified by Western Blotting to evaluate postsynaptic density and no significant changes were found between the levels of this protein in Tg(CaMKII-hA_{2A}R) (n=6) when comparing to WT littermates (n=6) (P>0.05) **(Figure 4.5)**.

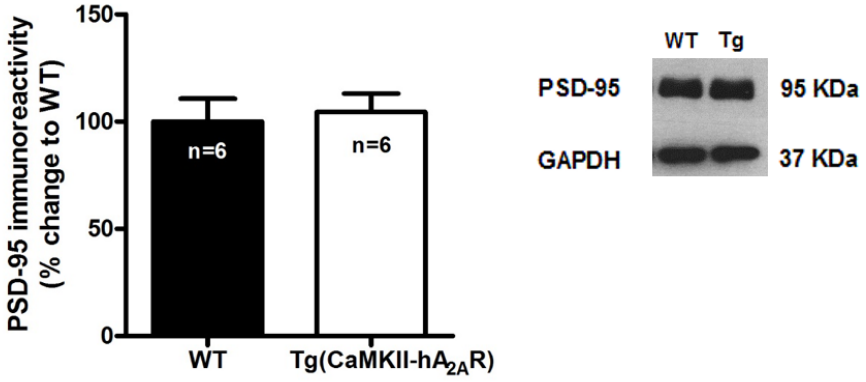

Figure 4.5 - PSD-95 levels in the rat hippocampus. Immunoreactivity of PSD-95 was measured in whole tissue homogenates either for WT (black) or Tg(CaMKII-hA_{2A}R) (white) animals. Specific immunoreactivity was normalized to that of GAPDH. Results are the mean ± SEM of six experiments. At the right, a representative image of the Western Blot is presented.

4.3 | Effects of $A_{2A}R$ overexpression in glial cell reactivity

Since noxious brain conditions and neurodegenerative processes are characterized by alterations in glial cell function, reactivity profile of microglia and astrocytes were evaluated in CaMKII-h$A_{2A}R$ transgenic model, in order to assess if neuronal-specific overexpression of $A_{2A}R$ drives changes in glial reactivity.

4.3.1 | Characterization of Microglial Phenotype

4.3.1.1 | Analysis of Iba1 immunoreactivity

Microglial reactivity was evaluated by Western Blotting through the levels of Iba1, a protein with a suggested role in calcium homeostasis that is known to be upregulated following microglial activation (Ito et al., 2001). Analysis of Iba1 reactivity **(Figure 4.6)** revealed an increase of 66.91 ± 24.77% ($P<0.05$) in the levels of this microglial activation marker in Tg(CaMKII-h$A_{2A}R$) rats (n=7) when comparing to WT littermates (n=7).

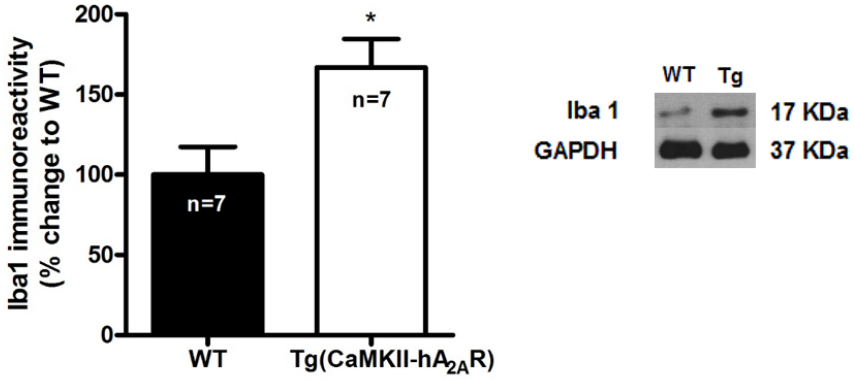

Figure 4.6 - Iba1 levels in the rat hippocampus. Immunoreactivity of Iba1 was measured in whole tissue homogenates either for WT (black) or Tg(CaMKII-h$A_{2A}R$) (white) animals. Specific immunoreactivity was normalized to that of GAPDH. Results are the mean ± SEM of seven experiments. At the right, a representative image of the Western Blot is presented. (*): $P<0.05$ calculated using an unpaired Student's t-test.

4.3.1.2 | Morphological analysis of microglial cells

Following the increase in microglial reactivity in Tg(CaMKII-h$A_{2A}R$) animals assessed by Western Blotting **(Figure 4.6)**, morphology of microglial cells was analysed in order to quantify differences in activation state **(Figure 4.7)**.

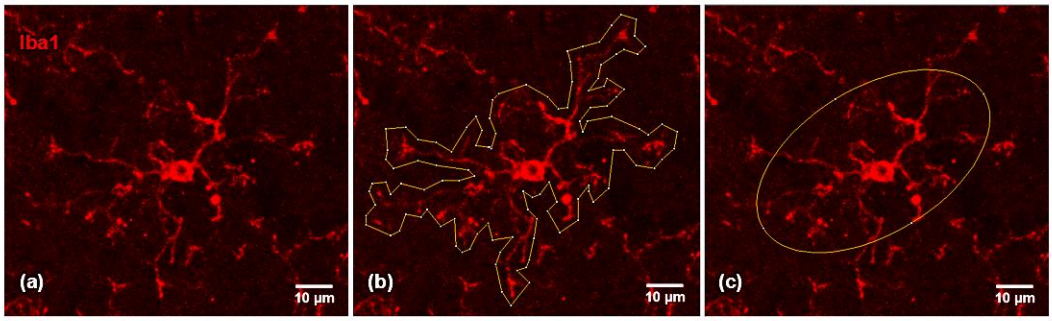

Figure 4.7 - Morphological analysis of microglial cells. A minimum of 60 representative Iba+ cells of CA1 area were randomly selected per animal (a). After drawing cell perimeter (b), tracing was fitted into an ellipse (c), allowing the quantification of the area of influence and shape of individual cells by measuring its parameters.

Microglial activation process is characterized by high morphological plasticity, consisting in a multistage morphological transformation from a ramified to amoeboid appearance, through the reduction of cell shape complexity and acquisition of characteristics resembling peripheral macrophages (Kettenmann et al., 2011). Therefore, the angle and area of the fitted ellipse were evaluated as a mean to infer about the shape of microglial cells.

Analysis of the area of the fitted ellipse revealed a significant decrease of $4{,}64 \times 10^8 \pm 5{,}134 \times 10^7$ μm^2 ($P<0.05$) in the area occupied by individual microglial cells of CA1 region in Tg(CaMKII-hA_{2A}R) rats (n=3) when comparing to WT littermates (n=2) **(Figure 4.8).**

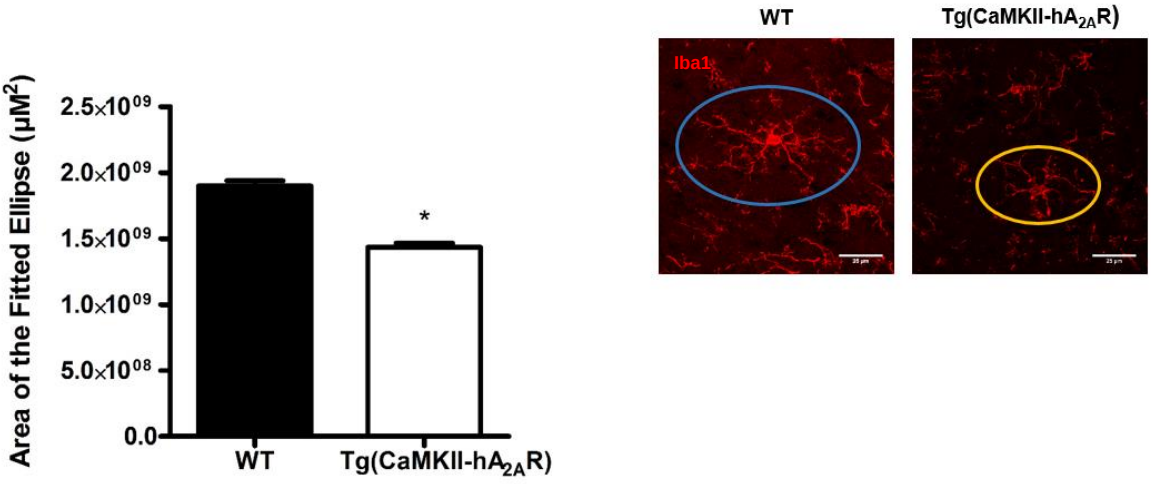

Figure 4.8 - Area occupied by individual microglial cells of CA1 area of hippocampus. A minimum of 60 representative Iba+ cells of CA1 area were randomly selected per each WT (black) (n=2) and Tg(CaMKII-hA_{2A}R) (white) (n=3) animals. Analysis was performed through the area of the ellipse fitted to each individual cell tracing. Results are presented as the mean ± SEM. At the right, representative images of the microglial phenotype are presented. Scale Bar: 25µm. (*): $P<0.05$ calculated using an unpaired Student's t-test.

In what concerns the analysis of the angle of the fitted ellipse, results revealed that microglial cells of CA1 area of Tg(CaMKII-hA$_{2A}$R) animals (n=3) have a less rounded shape when comparing to WT littermates (n=2), as indicated by a significant increase in ellipse elongation (16400 ± 6908) (P<0.05) **(Figure 4.9)**.

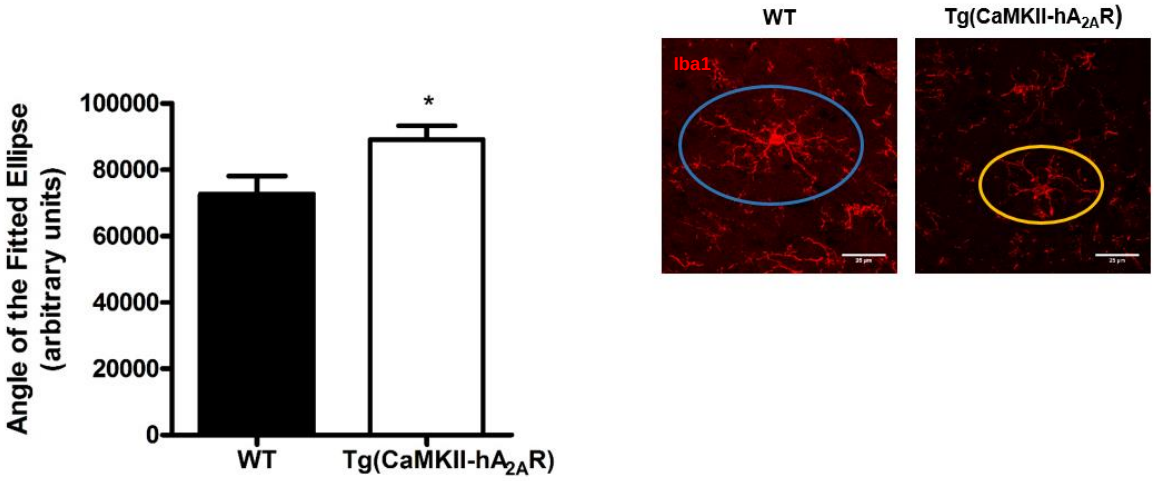

Figure 4.9 – Elongation of individual microglial cells of CA1 area of hippocampus. A minimum of 60 representative Iba+ cells of CA1 area were randomly selected per each WT (black) (n=2) and Tg(CaMKII-hA$_{2A}$R) (white) (n=3) animals. Analysis was performed through the angle of the ellipse fitted to each individual cell tracing. Results are presented as the mean ± SEM. At the right, representative images of the microglial phenotype are presented. Scale Bar: 25µm. (*): P<0.05 calculated using an unpaired Student's t-test.

4.3.1.3 | Microglial cell counts and CD11b expression levels

Increased expression of a binding protein for intracellular cell adhesion molecule-1 and complement C3bi (CD11b) has been correlated with the severity of microglial activation in several neuroinflammatory diseases (Roy et al., 2006). Therefore, hippocampal microglial cells in CaMKII-hA$_{2A}$R transgenic model were characterized by flow cytometry using CD11b as surface marker, quantifying both microglial population and its overall expression of CD11b.

The first approach consisted of a Percoll gradient, with the aim of establishing correct gatings for microglial cells using a purified sample. The population of interest was identified based on parameters of size/viability (FSC), granularity (SSC) and relative expression of CD11b (FL1) and CD45 (FL2) (CD45^{low}CD11b^{+}) **(Figure 4.10)**.

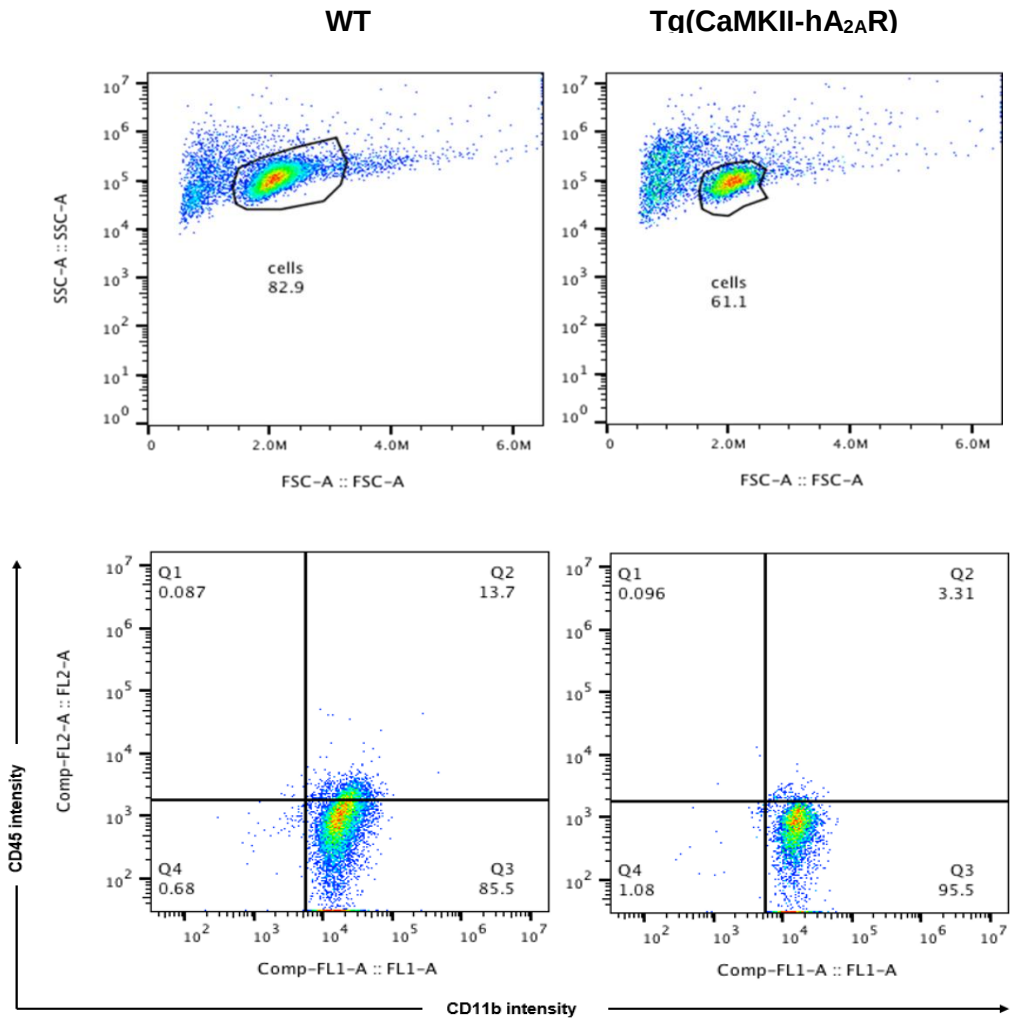

Figure 4.10 – Gating of microglial population for Flow Cytometry analysis. A Percoll gradient was performed with hippocampal tissue from WT and Tg(CaMKII-hA$_{2A}$R) animals (n=2). Cells were gated based on parameters of size/viability (FSC), granularity (SSC) and relative expression of CD11b (FL1) and CD45 (FL2) (CD45^{low}CD11b^{+}).

CD45 intensity in gated cells was lower than predicted, when assuming microglial phenotype as CD45^{low}CD11b^{+} **(Figure 4.10)**. In order to ensure correct isolation of the population of interest, CD45 antibody staining was tested using lymph node samples and proven not to be effective (**Supplementary Figure 7.6**). Consequently, the presence of macrophages and monocytes (CD45^{high}CD11b^{+}) in our isolated cell population could not be entirely excluded. However, since microglia are considered to be the only cells that express CD11b in intact brain, due to the absence of leukocytes infiltrating brain tissue (Jeong et al., 2013), we assumed CD11b^{+} cells as our population of interest.

Therefore, in order to perform a quantitative analysis of total microglial cell number in the hippocampus, previous gating was applied in non-purified samples and the total number of CD11b+ cells per 650000 total scanning events was analysed. No significant differences were found in total CD11b+ cell number between Tg(CaMKII-hA$_{2A}$R) (n=2) and WT littermates (n=2) (P>0.05) **(Figure 4.11)**.

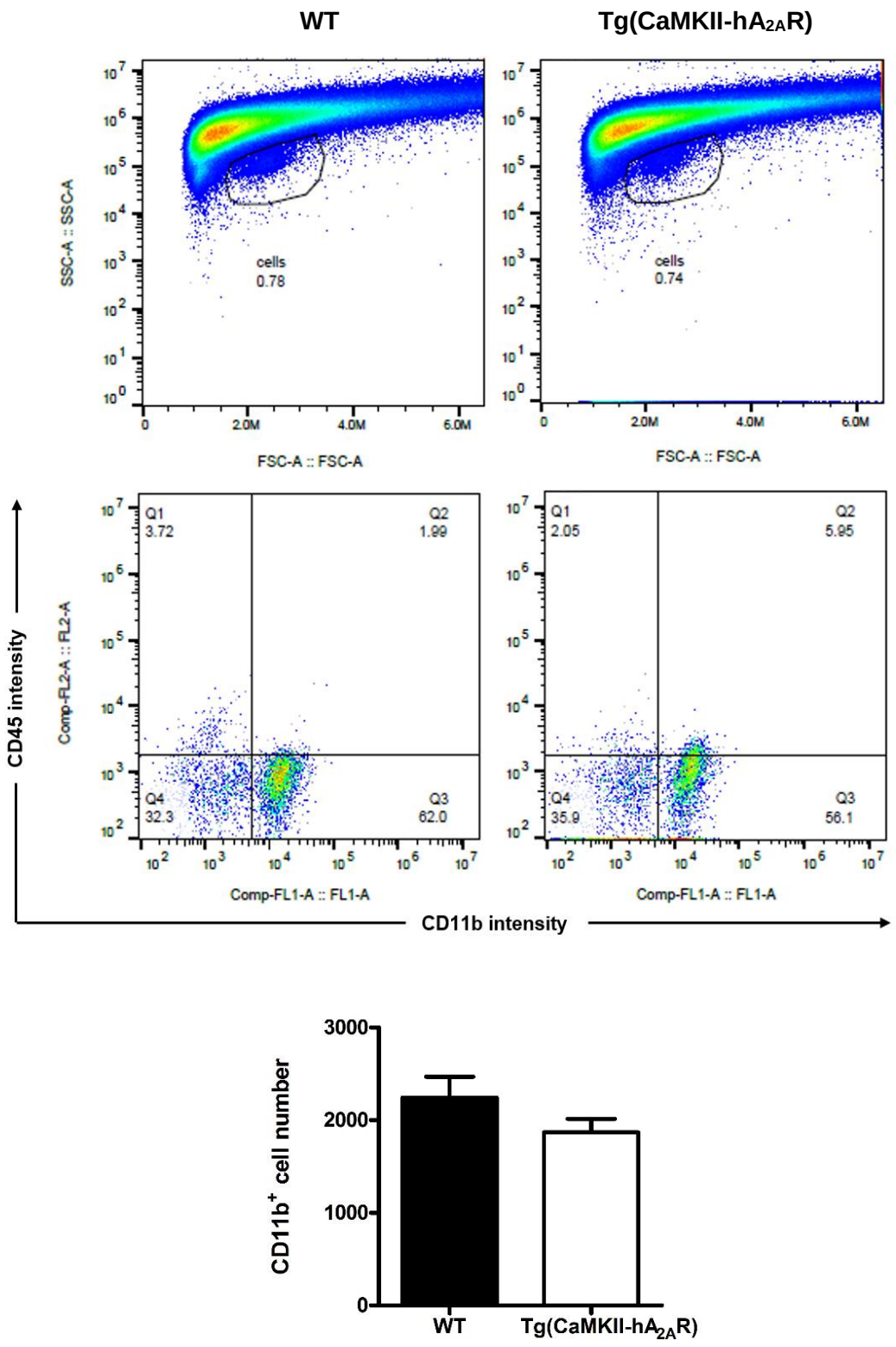

Figure 4.11 – CD11b$^+$ cell number in the hippocampus. Non-purified hippocampal samples from WT and Tg(CaMKII-hA_{2A}R) animals (n=2). Cells were gated based on parameters of size/viability (FSC), granularity (SSC) and relative expression of CD11b (FL1) and CD45 (FL2) (CD45^{low}CD11b$^+$). Results are presented as the mean ± SEM, per 650000 total scanning events.

In what concerns the overall expression of CD11b fluorescence, no significant differences were found in CD11b Median Fluorescence Intensity between Tg(CaMKII-hA$_{2A}$R) (n=2) and WT littermates (n=2) (P>0.05) **(Figure 4.12)**.

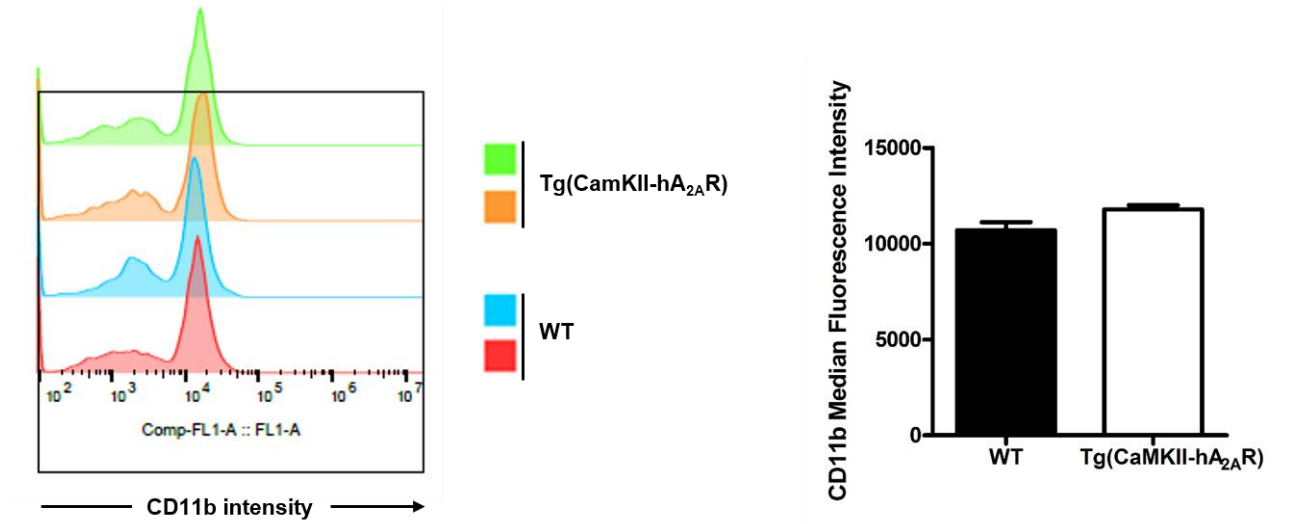

Figure 4.12 – CD11b Fluorescence Intensity. Non-purified hippocampal samples from WT and Tg(CaMKII-hA$_{2A}$R) animals (n=2). Cells were gated based on parameters of size/viability (FSC), granularity (SSC) and relative expression of CD11b (FL1) and CD45 (FL2) (CD45^{low}CD11b^{+}). At the left, histogram of CD11b Fluorescence Intensity in WT and Tg(CaMKII-hA$_{2A}$R) samples (n=2). At the right, results are presented as the mean ± SEM of the CD11b Median Fluorescence Intensity (n=2).

4.3.2 | Characterization of Astroglial Phenotype

4.3.2.1 | Analysis of GFAP immunoreactivity

Astrocytic reactivity was assessed using the levels of GFAP, a member of the intermediate filament family of proteins suggested to be involved in the control of shape, movement and function of astroglial cells (Eng et al., 2000) that is overexpressed following their activation. Immunoblot analysis revealed a significant decrease of 20.76 ± 8.019% (P<0.05) in GFAP protein levels of Tg(CaMKII-hA$_{2A}$R) rats (n=7) when comparing to WT littermates (n=7) **(Figure 4.13)**.

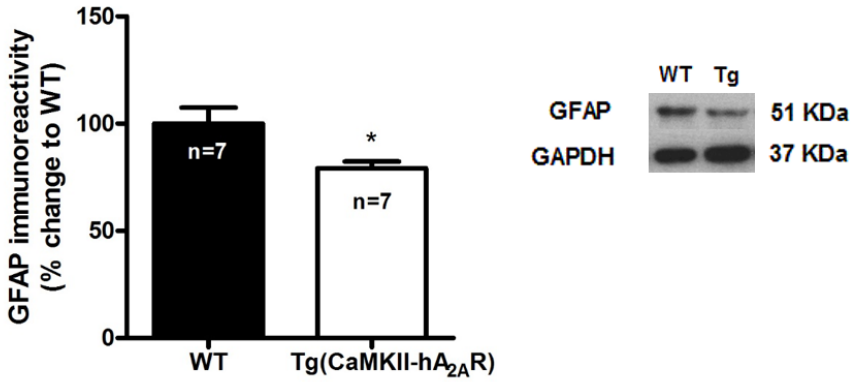

Figure 4.13 - GFAP levels in the rat hippocampus. Immunoreactivity of GFAP was measured in whole tissue homogenates either for WT (black) or Tg(CaMKII-hA_{2A}R) (white) animals. Specific immunoreactivity was normalized to that of GAPDH. Results are the mean ± SEM of seven experiments. At the right, a representative image of the Western Blot is presented. (*): P<0.05 calculated using an unpaired Student's t-test.

4.3.2.2 | Morphological Analysis of Astroglial Cells

Overall morphology of hippocampal astrocytes was evaluated by GFAP immunohistochemistry, in order to investigate if A_{2A}R overexpression in forebrain neurons had influence on the density, distribution and phenotype of astroglial cells.

No apparent changes were found in overall astroglial phenotype by GFAP immunohistochemistry **(Figure 4.14)**.

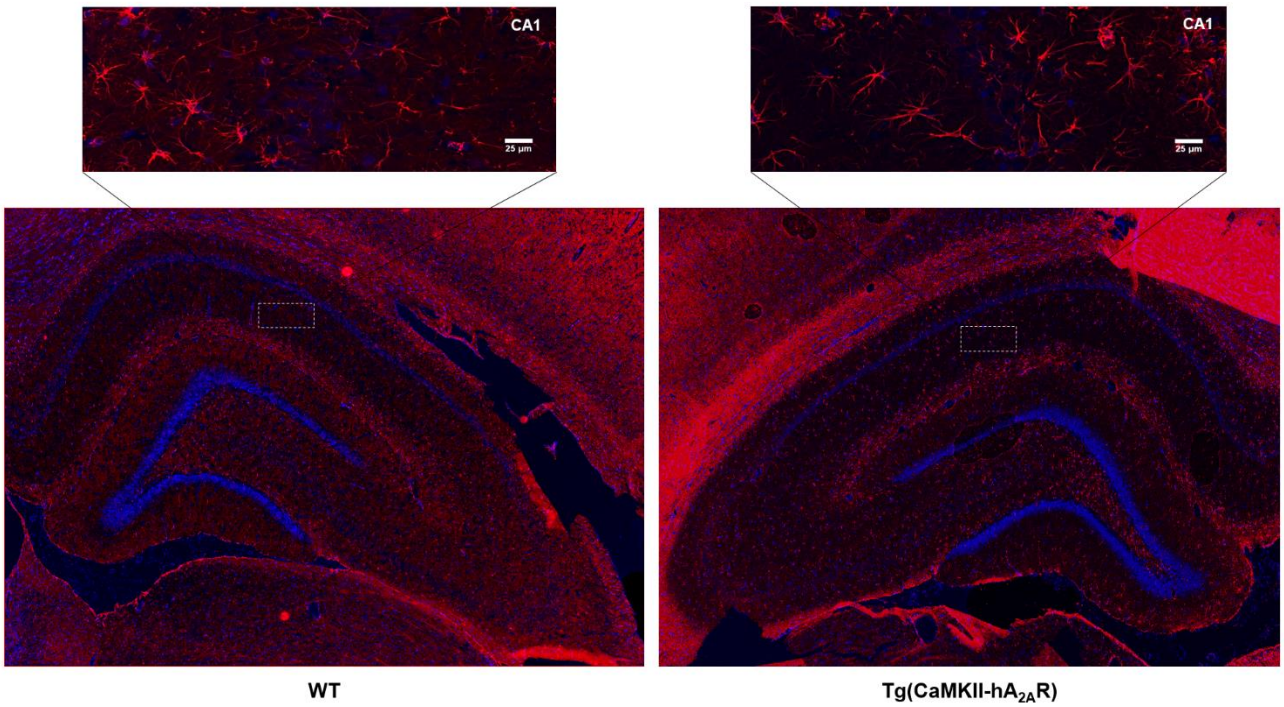

Figure 4.14 - Overall astroglial phenotype in hippocampus. Fluorescence immunohistochemistry composition of hippocampus of WT and Tg(CaMKII-hA_{2A}R) animals at 10x magnification. At the top, representative images of astroglial phenotype at CA1 area of hippocampus are presented. Scale Bar: 25µm. Neuronal nuclei are stained with Hoechst (blue) and astrocytes are identified by red fluorescence using mouse anti-GFAP antibody (Millipore).

A detailed assessment of astrocytic morphology was then performed by Sholl Analysis of GFAP+ cells of CA1 area, stained by DAB immunohistochemistry. No significant changes were detected in length and complexity of astroglial processes, between Tg(CaMKII-hA_{2A}R) (n=3) and WT littermates (n=2) (P>0.05) (Figure 4.15).

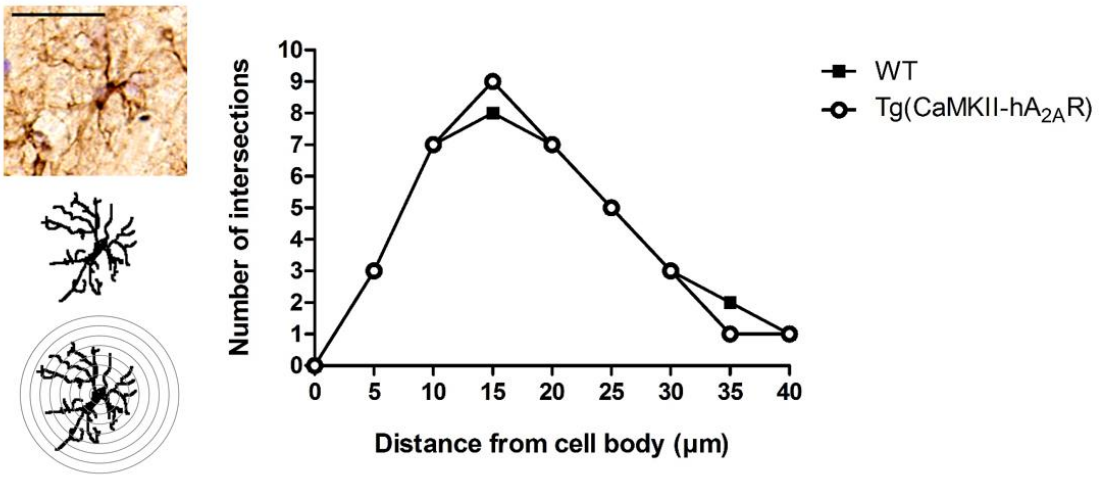

Figure 4.15 - Length and complexity of astroglial processes in CA1 area. Morphology of 90 GFAP+ cells from each WT (black) (n=2) and Tg(CaMKII-hA_{2A}R) (white) (n=3) animals was evaluated by Sholl Analysis. Results are the mean of process intersections per each concentric ring distributed at equal distances from cell body. Left panel: representative images of the method. Scale Bar: 40µm.

5 | DISCUSSION

This study aimed **to evaluate the impact on astrocytes and microglia of the pathological phenomena associated with A_{2A} receptors dysregulation in the hippocampus.**

Our main findings show that $A_{2A}R$ overexpression conditional to the glutamatergic forebrain neurons - that mimics the long-term robust upregulation induced by noxious brain conditions - is sufficient to induce microglial activation and reduction of astroglial reactivity, resembling features of aging process. This corroborates the view of a modulatory potential of adenosine in the functional control of different cell subsets

5.1 | Localization of human $A_{2A}R$ overexpression in the rat hippocampus

It was confirmed that Tg(CaMKII-h$A_{2A}R$) animals overexpress the human $A_{2A}R$ in CA3 axonal projections and in the neuropil of DG and CA1 hippocampal areas. Further analysis with Electron Microscopy using neuronal markers would be useful, in order to evaluate the localization of $A_{2A}R$ overexpression with a higher resolving power.

The homology between human $A_{2A}R$ and rat $A_{2A}R$ is about 84-85%, with receptors being functionally similar, activated by endogenous adenosine and coupled to a G_s protein (Giménez-Llort et al., 2007). Functional significance of human $A_{2A}R$ overexpressed in the rat is demonstrated by the results of the synaptic transmission characterization performed by our group.

Tg(CaMKII-h$A_{2A}R$) model allowed the confirmation of the hypothesis that $A_{2A}R$ upregulation in neurons is sufficient to drive synaptic dysfunction and cognitive impairment in a mechanism that mimics hippocampal aging (Temido-Ferreira et al., 2015).

5.2 | Neuronal $A_{2A}R$ overexpression induced alterations in microglia

Overall, results of microglial cell characterization pointed towards a difference in microglial phenotype between Tg(CaMKII-h$A_{2A}R$) animals and WT littermates that may reflect alterations in activation profile (**Figure 5.1**).

Microglial phenotype of Tg(CaMKII-h$A_{2A}R$) animals consisted of cells with higher elongation, decreased area of influence, shorter ramifications, and increased Iba1 immunoreactivity, suggesting that neuronal-specific overexpression of $A_{2A}R$ induces a primed state of microglia, triggering morphological alterations that resemble early stages of activation process.

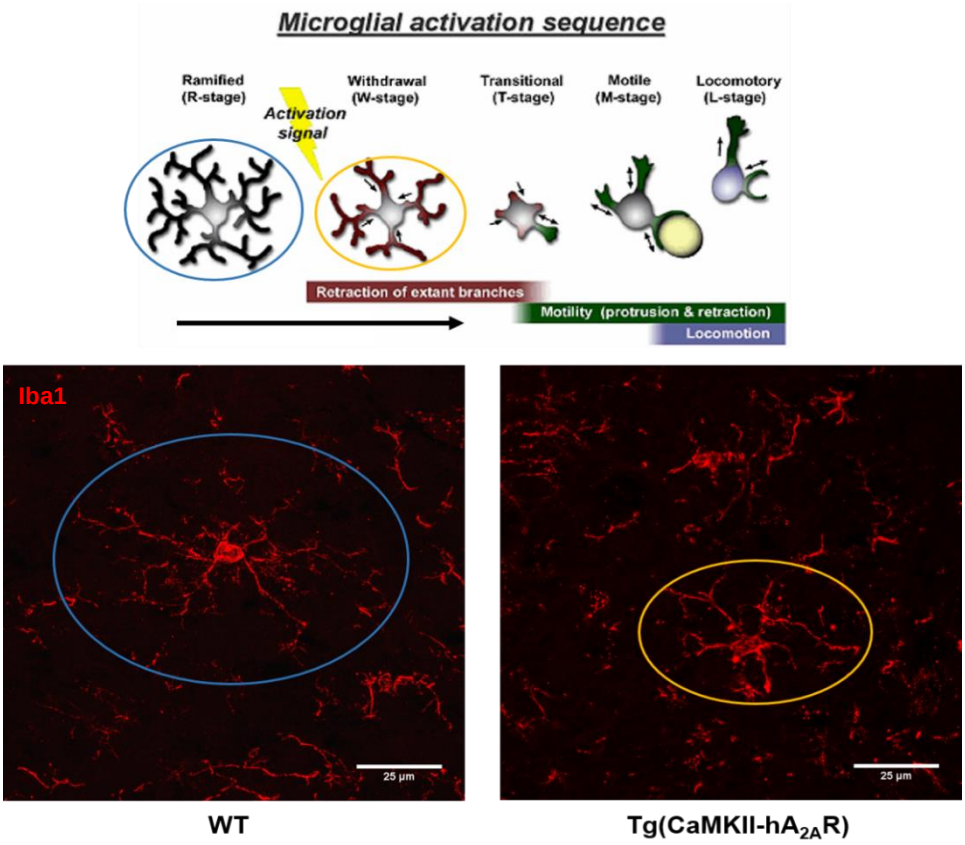

Figure 5.1 – Representative images and schematic representation of differences in microglial phenotype. Representative fluorescence images of microglial cells from CA1 area of WT and Tg(CaMKII-hA_{2A}R) hippocampal sections at 63x magnification. Microglia are identified by red fluorescence using goat anti-Iba1 antibody (Abcam). At the top, a schematic representation of Microglial activation sequence (adapted from http://bioweb.biology.uiowa.edu/daileylab/projects.html)

Since precise detection of different stages of activation process through morphologic analysis is one of the major challenges in microglial research (Das Sarma et al., 2013), combined histological and flow cytometry analysis are crucial to perform a full phenotypic characterization, taking the differential expression of surface markers into account.

Although increased CD11b expression is known to be associated with microglial activation (Roy et al., 2006), in current study Iba1 upregulation is not correlated with an increase in CD11b expression levels. However, as characterization was performed under basal conditions, such activated phenotype is not expected to occur in a physiological context, with substantial pathology being required to take microglia into a higher state of activation, in order to increase CD11b expression. Moreover, several studies have considered Iba1 a better marker for morphological differentiation (Das Sarma et al., 2013), since it has major roles in calcium signalling, RacGTPase activation and membrane ruffling, important features in macrophage activation (Kanazawa et al., 2002).

Chronic microglial activation is an important component of neurodegenerative diseases, contributing to CNS dysfunction and injury (González-Scarano & Baltuch, 1999). Aging process - strongest risk factor for neurodegeneration - is characterized by a significant increase in microglial activation, together with an upregulation of genes related to cellular stress and inflammation, as well as a decrease of growth factors and trophic support (reviewed in Lucin & Wyss-Coray, 2009). Accordingly, microglia derived from aged mice show process retraction and increased basal production of proinflammatory mediators, namely TNFα, IL-1β and IL-6, reflecting a hypersensitive preconditioned state, that causes a more rapid and pronounced response upon any insult, creating an inflammatory microenvironment which promotes degeneration (Olah et al., 2011).

The molecular pathways underlying microglial-induced neuroinflammation gain relevance since several studies have described a potential role of microglia in plasticity and function of synaptic circuits in the mature CNS, associating soluble factors released by microglia and actions upon basal transmission and synaptic plasticity (reviewed in Schafer et al., 2013). Electrophysiology studies with microglial-conditionated medium have demonstrated a potentiation of NMDA receptor-mediated postsynaptic responses (Moriguchi et al., 2003) and enhancement of LTP (Hayashi et al., 2006) as well as modulation of basal glutamatergic transmission (Pascual et al., 2012), reinforcing the functional significance of microglial activation and paracrine signalling on synaptic activity, having IL-1β (Nisticò et al., 2013; Simões et al., 2012), glycine, L-serine (Hayashi et al., 2006) and ATP (Pascual et al., 2012) as principal molecular mediators.

Therefore, current results corroborate the hypothesis of $A_{2A}R$ dysregulation as an early-aging mechanism in the hippocampus, with a microglial primed phenotype that may contribute for the alterations of synaptic transmission observed in Tg(CaMKII-h$A_{2A}R$) animals (Temido-Ferreira et al., 2015), mimicking features of aging process. It suggests that once neuronal-specific $A_{2A}R$ overexpression triggers a primed/preconditionated microglial state, it may favour the secretion of proinflammatory factors that can damage neurons and alter synaptic transmission, promoting the establishment of a chronic microenvironmental alteration. This, in turn, would lead to the subsequent activation of microglia, enhancing neuroinflammatory status and leading to a self-perpetuating cycle that would, ultimately, lead to neurodegeneration.

Moreover, different brain insults also cause an upregulation of the expression and density of $A_{2A}R$ in activated microglia (Canas et al., 2004; Yu et al., 2008). *In vitro* and *in vivo* studies clearly demonstrate that $A_{2A}R$ controls several important functions operated by microglia, mediating process retraction (Gyoneva et al., 2014; Orr et al., 2009), synthesis and release of inflammatory mediators, levels of inflammatory enzymes and proliferation (Santiago et al., 2014). As such, although $A_{2A}R$ effects have been attributed to actions in neuronal receptors, blockade of microglial $A_{2A}R$ might also yield neuroprotection through direct actions in this cellular subset. Furthermore, the vicious loop

caused by a chronic shift of microenvironment towards inflammation in Tg(CaMKII-hA_{2A}R) animals might concomitantly result from the activation of microglial A_{2A}R.

All gathered, results point towards the therapeutic interest of identifying regulatory systems capable of rebalancing microglial function in the management of the progression of neurodegenerative diseases.

5.3 | Neuronal A_{2A}R overexpression induced alterations in astrocytes

Results of astroglial cell characterization indicate that neuronal-specific A_{2A}R overexpression induces alterations in astrocytic reactivity by decreasing GFAP immunoreactivity, without influencing the density, distribution and morphology of astroglial cells.

Factors reducing astrocyte activation, as measured by the expression levels of GFAP, have not been sufficiently studied (Pekny et al., 2016). Early stages of neurodegenerative diseases are characterized by an asthenic phenotype of astroglial cells, with substantial loss of function (Verkhratsky et al., 2015).

Among many homeostatic functions, astrocytes have an important role in supporting synaptic transmission, namely by regulating ion concentrations in the synaptic cleft, providing energetic metabolites to neurons, performing the uptake of neurotransmitters and supplying neuronal terminals with glutamine, an obligatory precursor for glutamate and GABA (Pekny et al., 2016). Therefore, astroglial loss of function is directly connected to the reduction of homeostatic support, having detrimental effects on the multipartite synapse.

Particularly, the accumulation of extracellular glutamate and consequent excitotoxicity phenomena contribute directly to the establishment and progression of most neurodegenerative diseases, highlighting the impact of glutamate transporters in the control of synaptic plasticity (Benarroch, 2010). Interestingly, GFAP expression was found to be required for the accurate expression and trafficking of astrocytic (EAAT1) and neuronal (EAAT2) glutamate transporters, with the loss of this intermediate filament protein resulting in an overall decrease in glutamate transport (Hughes et al., 2004). LTP/LTD probability is highly dependent on synaptic glutamate concentrations, thus, an impairment in the uptake of this neurotransmitter resulting from an asthenic astrocytic phenotype could contribute to the alterations in synaptic transmission observed in Tg(CaMKII-hA_{2A}R) animals (Temido-Ferreira et al., 2015).

Moreover, astroglial asthenia has been described in various forms of neuropathology, from psychiatric to neurodegenerative diseases. Studies on mood disorders correlate specific deficits in GFAP expression in corticolimbic circuits with depressive-like behaviour in animal models (Gosselin et al., 2009) and Major Depression Disorder in humans (Si et al., 2004). Little is yet known on the aetiology of this correlation, remaining the speculation on whether the astroglial defect is the cause

or a direct consequence of anxiety and stress. Nonetheless, it has also been demonstrated that paradigms of chronic stress (Imbe et al., 2012; Tynan et al., 2013) and chronic unpredictable mild stress (Ye et al., 2011) also selectively decreased GFAP expression, without reducing astrocytic numbers and specific pharmacological ablation of astrocytes induces a depressive-like behaviour similar to that observed following chronic stress (Banasr & Duman, 2007).

In aging, experimental data is still controversial, and aging effects on astroglial physiology remain generally unknown, with both increase in astroglial reactivity and astrocytic senescence being reported in aged animals (reviewed in Rodríguez-Arellano et al., 2015).

Since Tg(CaMKII-hA_{2A}R) animals display altered exploratory behaviour, anhedonic-like phenotype and increased behavioural despair - key features of depressive-like behaviour (Coelho et al., 2014) that are in line with the depressive signs found in aging, chronic stress and AD, a link is suggested between forebrain A_{2A}R overexpression and a functional disruption of astroglial cells.

On the other hand, although the actions of A_{2A}R have mainly been assumed to result from the activation of neuronal A_{2A}R, this type of receptor is also present in astrocytes, mediating glucose metabolism, astrogliosis, proliferation, cellular volume and the release of neurotrophic factors and interleukins (reviewed in Boison et al., 2010 and Daré et al., 2007).

Orr et al. (2015) concluded that astrocytic A_{2A}R regulate memory and may mediate aberrant effects under pathological conditions, by modulating processes underlying memory storage or consolidation, such as synaptic plasticity and neural network activity. Coincidentally, it is also known that the activation of astrocytic A_{2A}R decreases the uptake of glutamate by inhibiting the activity and expression of EEAT1 and EAAT2 (Matos et al., 2012). Therefore, our results suggest that the features of depressive-like behaviour (Coelho et al., 2014), memory impairments and synaptic alterations (Temido-Ferreira et al., 2015) that characterize Tg(CaMKII-hA_{2A}R) model might be partially seen as a consequence of the loss of astroglial function driven by neuronal-specific A_{2A}R overexpression and may also involve activation of astroglial A_{2A}R.

Furthermore, by suggesting that astrocytes influence the pathophysiology of A_{2A}R dysregulation, the results highlight the therapeutic interest of modulating astrocytic function in pathological conditions.

6 | CONCLUSIONS

In conclusion, our results prove the ability of neuronal-specific $A_{2A}R$ overexpression to impact on glial cell function. $A_{2A}R$ dysregulation underlying synaptic dysfunction and cognitive impairments in Tg(CaMKII-h$A_{2A}R$) model derives from a synergy of synaptic and glial dysfunction, resembling features of hippocampal aging (summarized in **Figure 6.1**).

The present results contribute to acknowledge neurocentrism as an obsolete theory in the study of neurological diseases, highlighting the importance of considering neurodegeneration as a consequence of homeostatic failure, giving relevance to the molecular and cellular changes in glia as well as neurons, when trying to decipher the mechanisms leading to neuropathology.

Also the current study suggests $A_{2A}R$ as a promising pharmacological target in neurodegenerative diseases, allowing a multifactorial approach with the aim of slowing down their progression.

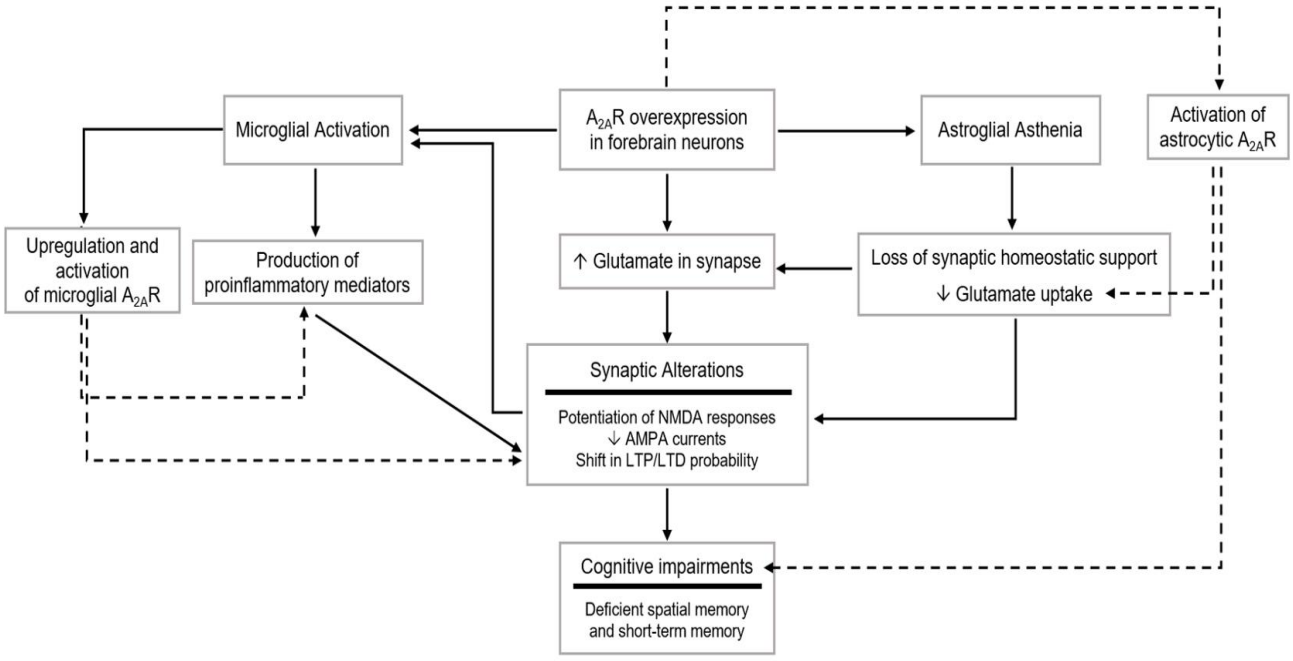

Figure 6.1 – Schematic representation of functional interrelations between neuronal, microglial and astrocytic phenotypes in Tg(CaMKII-h$A_{2A}R$) model. Broken arrows indicate connections that are not fully characterized. Relevant references: Benarroch, 2010, *Neurology*; Hughes et al., 2004, *Brain Res Mol Brain Res;* Matos et al., 2012, *Glia;* Orr et al., 2015, *Nat Neurosci.;* Orr et al., 2009, *Nat Neurosci.;* Pekny et al., 2016, *Acta Neuropathol.;* Santiago et al., 2014, *Mediators Inflamm.;* Schafer et al., 2013, *Glia;* Temido-Ferreira et al., 2015; Verkhratsky et al., 2015, *Neuroscientist.*

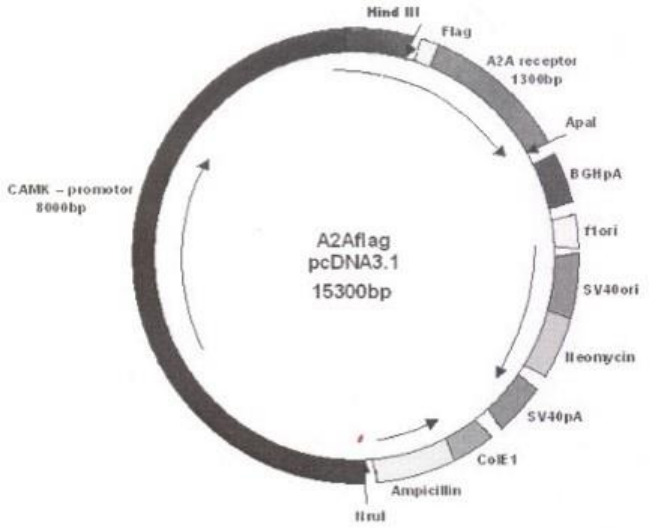

Supplementary Figure 7.1 – DNA construct used to generate Tg(CaMKII-hA_{2A}R) rats. Construct consists of a full-length human A2A cDNA cloned into an expression vector with the 8.5kb mouse CaMKIIα promoter and a polyadenylation cassete of bovine growth hormone. (Michael Bader, MDC, Berlin).

Primer CamKII (Forward)

Primer hA2AR (Reverse)

Human A2AR

FLAG epitope

```
  1 GACTAAGTTT GTTCGCATCC CCTTCTCCAA CCCCCTCAGT ACATCACCCT
 51 GGGGGAACAG GGTCCACTTG CTCCTGGGCC CACACAGTCC TGCAGTATTG
101 TGTATATAAG GCCAGGGCAA AGAGGAGCAG GTTTTAAAGT GAAAGGCAGG
151 CAGGTGTTGG GGAGGCAGTT ACCGGGGCAA CGGGAACAGG GCGTTTCGGA
201 GGTGGTTGCC ATGGGGACCT GGATGCTGAC GAAGGCTGTC GACGCTGTGA
251 GCAGCCACAG TGCCCTGCTC AGAAGCCCCA AGCTTGGTAC CGAGCTCGGA
301 TCCACTAGTA ACGGCCGCCA GTGTGCTGGA ATTCATGCCC ATCATGGGCT
                                    M  P  I  M  G  S    Frame 2
351 CCGATTACAA AGACGATGAC GATAAATCGG TGTACATCAC GGTGGAGCTG
      D  Y  K  D  D  D  D  K  S  V  Y  I  T  V  E  L    Frame 2
401 GCCATTGCTG TGCTGGCCAT CCTGGGCAAT GTGCTGGTGT GCTGGGCCGT
    A  I  A  V  L  A  I  L  G  N  V  L  V  C  W  A  V    Frame 2
451 GTGGCTCAAC AGCAACCTGC AGAACGTCAC CAACTACTTT GTGGTGTCAC
      W  L  N  S  N  L  Q  N  V  T  N  Y  F  V  V  S  ?  Frame 2
```

Supplementary Figure 7.2 – Sequence of the 450bp PCR product specific for Tg(CaMKII-hA_{2A}R). FLAG-tag is in frame with hA_{2A}R and inserted between the 6th and 7th aminoacids of the N-terminal of transgenic human A_{2A}R protein.

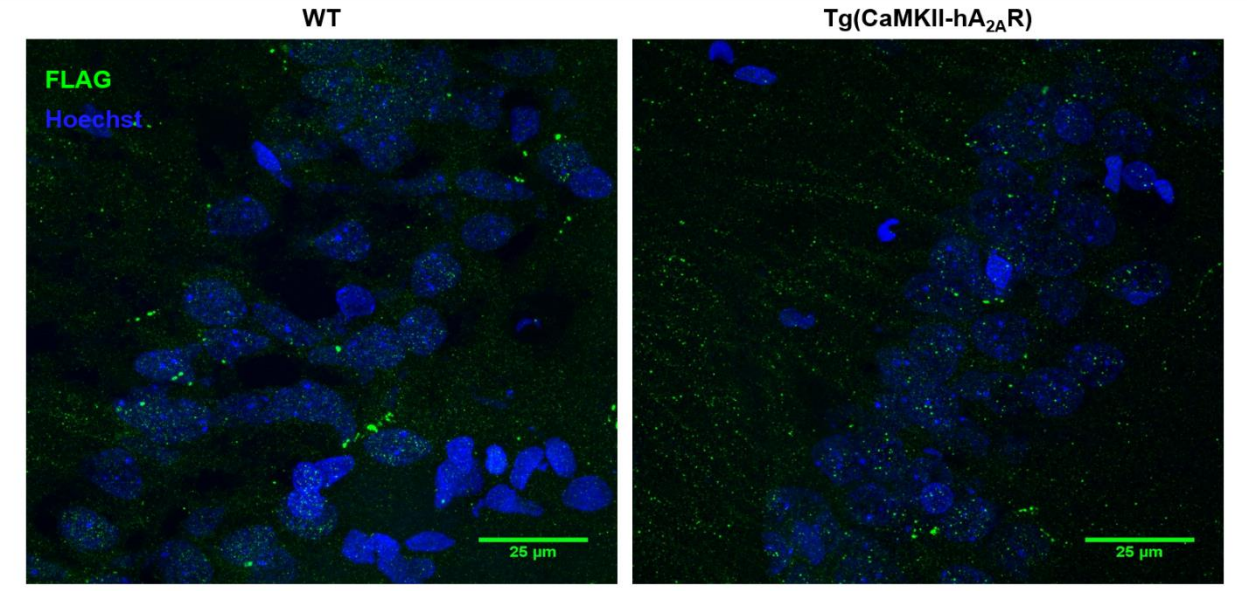

Supplementary Figure 7.3 - FLAG staining by immunohistochemistry. Fluorescence immunohistochemistry images from CA1 area of 12µm rat hippocampal sections at 63x magnification. Neuronal nuclei are stained with Hoechst (blue) and FLAG is identified by green fluorescence using rabbit anti-FLAG antibody (Sigma-Aldrich). Scale Bar: 25µm.

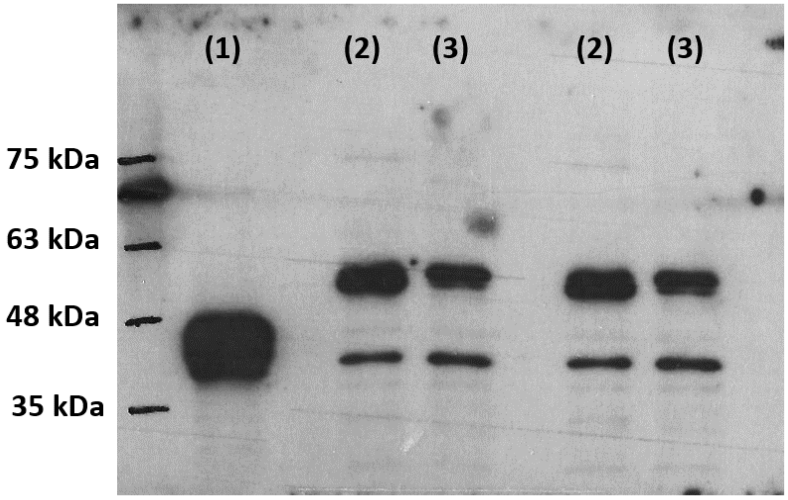

Supplementary Figure 7.4 - Rabbit anti-FLAG antibody (Sigma-Aldrich) staining profile by Western Blotting Analysis. Staining profile and specificity were evaluated by Western Blotting analysis, using a protein sample containing a FLAG-tag as a positive control (2µg) (1), and whole tissue hippocampal homogenates from a Wistar rat (WT) (2) and a Tg(CaMKII-hA$_{2A}$R) animal (3) (20µg).

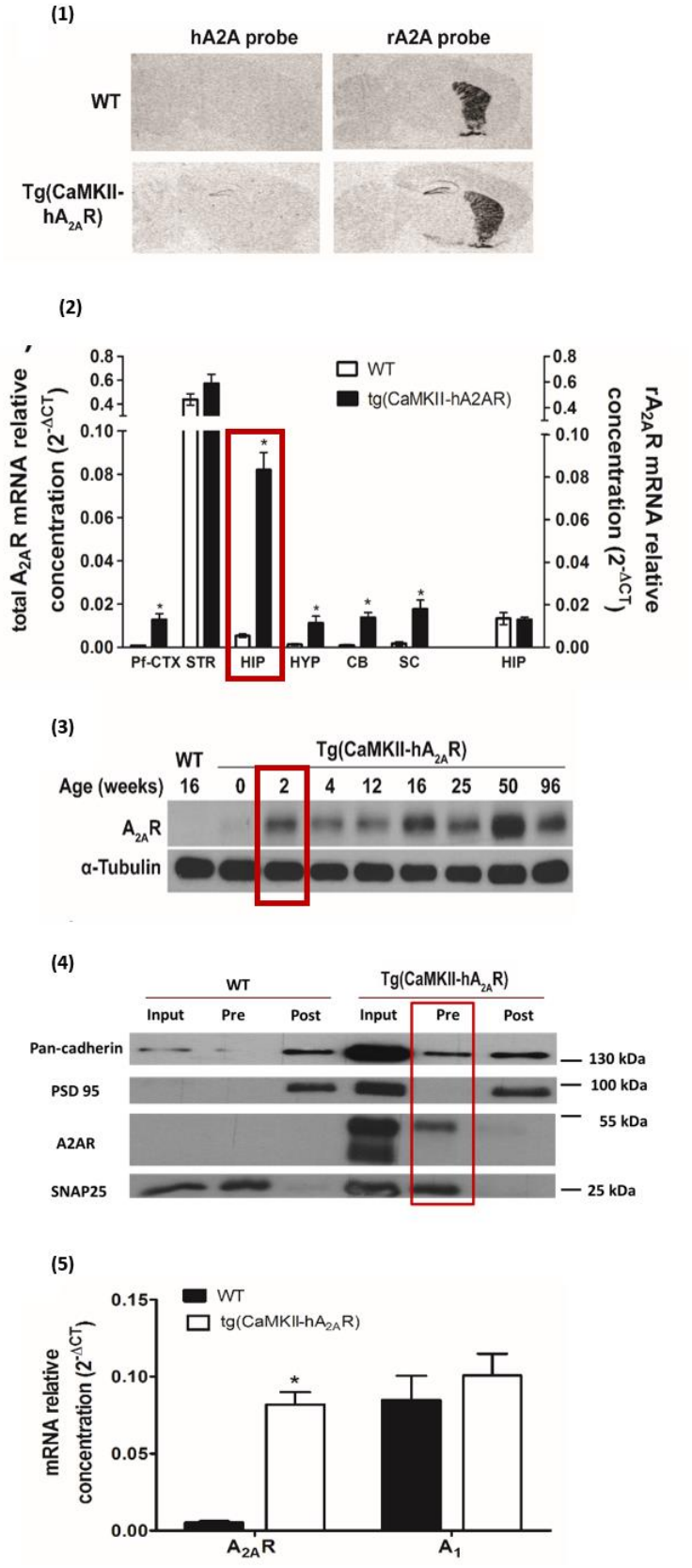

Supplementary Figure 7.5 – Molecular Features of CaMKII-hA$_{2A}$R overexpression. Tg(CaMKII-hA$_{2A}$R) animals show an A$_{2A}$R overexpression in the forebrain, evaluated by *in situ* hybridization (1) and confirmed by qPCR (2). A$_{2A}$R protein levels increase from 2 weeks-old onwards in the hippocampus (3), in the pre-synaptic region (4), without affecting A$_1$R levels (5). Results were analysed using unpaired Student's t-test for each gene/brain area, (*) P<0.05 compared to WT. (Lopes et al, unpublished)

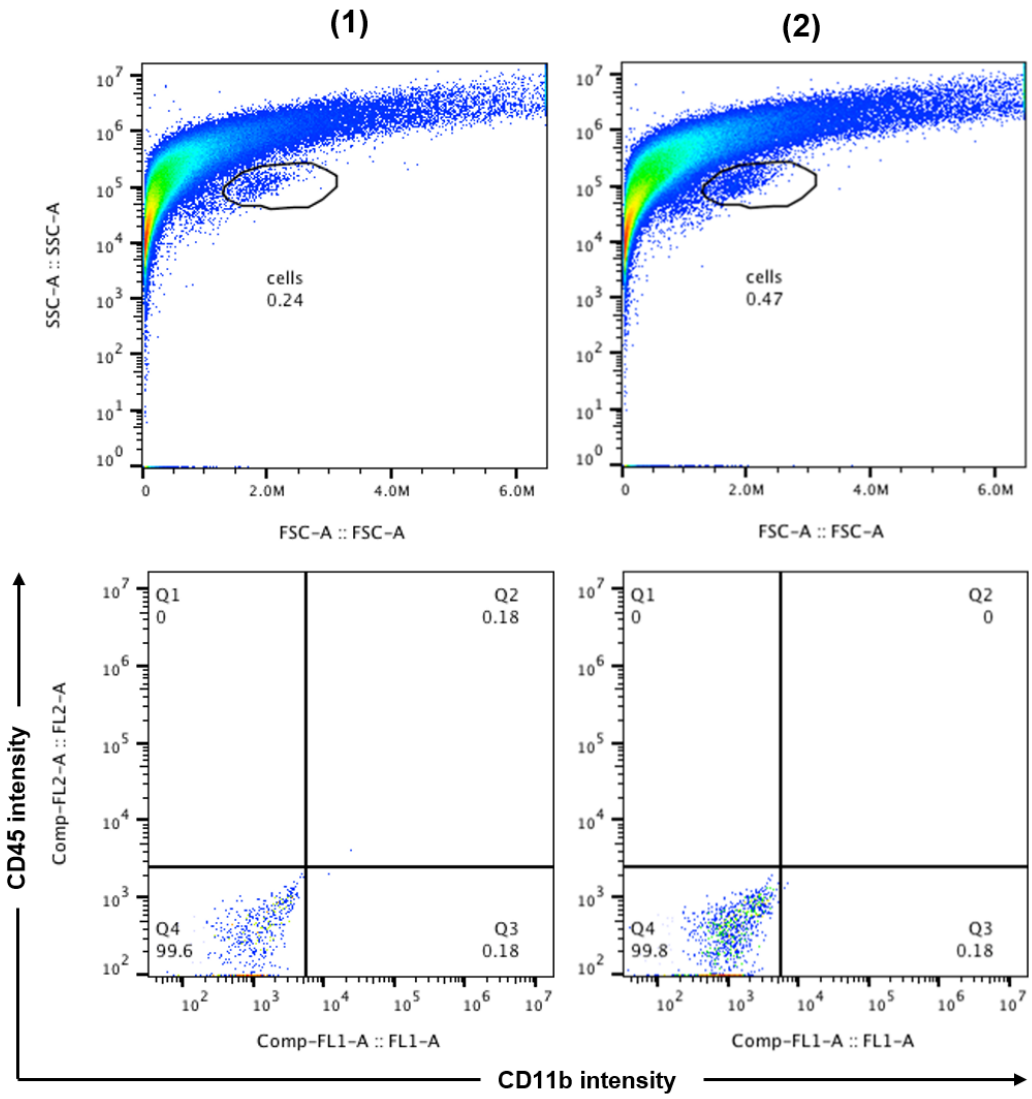

Supplementary Figure 7.6 – Flow Cytometry Analysis of CD45 antibody staining profile in rat lymph node sample. Unstained sample (1); sample stained with PE-conjugated anti-CD45 (OX30) antibody (Santa Cruz Biotechnologies) and FITC-conjugated anti-integrin αM/CD11b (OX42) antibody (Santa Cruz Biotechnologies) at 1:200 concentration (2). Cells were gated based on parameters of size/viability (FSC), granularity (SSC).

8 | ACKNOWLEDGEMENTS

No final desta etapa de grande crescimento profissional e pessoal, não posso deixar de agradecer a todos os que - directa ou indirectamente - contribuíram para que esta dissertação fosse possível:

Às minhas orientadoras, pela simpatia, amizade e toda a ajuda e motivação ao longo desta jornada, sobretudo quando a frustração teimava em ser palavra de ordem. Um imenso obrigada por me darem o privilégio de dar os primeiros passos em investigação científica sabendo que não poderia ter escolhido melhor.

À Luísa, pelo voto de confiança ao receber-me no seu grupo, por todos os ensinamentos e valiosos momentos de discussão científica, por ser para mim um exemplo na ciência e fora dela.

À Joana, pela paciência, cumplicidade, preocupação e carinho demonstrados diariamente, que não me deixaram esmorecer perante os vários desafios com que nos fomos deparando. Obrigada por todos os conhecimentos, ideias e brainstormings e por me teres sempre dado espaço para pensar e evoluir.

Aos colegas de laboratório que me receberam de braços abertos e me fazem sentir de coração cheio por pertencer a um grupo definido pelo verdadeiro espírito de equipa.

Ao Rui, por tudo o que me ensinou, por ser incansável e estar sempre disponível para juntar ciência e uma boa dose de gargalhadas.

À Mariana, Diana, Miguel e Vânia, por toda a disponibilidade e ajuda, aliadas a uma imensa cumplicidade, que fizeram com que o laboratório fosse muito mais do que um local de trabalho. Obrigada por trocarem o desespero por sorrisos e serem, mais do que colegas, amigos.

Às várias pessoas que me comprovaram que a simpatia, entreajuda e partilha de conhecimentos são o motor do sucesso.

Ao Biotério de Roedores (IMM) pelo apoio na manutenção da colónia.

À Unidade de Bioimagem (IMM), particularmente ao José Rino, Ana Nascimento e António Temudo, por toda a disponibilidade e ajuda com a aquisição e análise de imagens.

À Julie Ribot e Pedro Papotto (Bruno Silva-Santos Lab) e Ana Vieira (Unidade de Citometria de Fluxo, IMM), pela preciosa ajuda com o mundo da citometria de fluxo.

À Tânia Carvalho (Laboratório de Histologia e Patologia Comparada, IMM) e ao Pedro Pereira (Serviço de Neuropatologia, Hospital Santa Maria) pela ajuda relacionada com a histologia.

Ao André Bastos (CEDOC, UNL) pela ajuda no processo de preparação de neurónios dissociados.

À Mariana, por estares comigo desde o primeiro momento desta tão importante etapa, pelo carinho e forte amizade e por acreditares mais em mim do que eu própria.

Ao Jorge, por estares incondicionalmente ao meu lado, partilhando comigo todas as alegrias e frustrações, e por apesar das ausências, faltas e maus humores fazeres sempre um esforço para beber do entusiasmo que sinto pela ciência.

Ao Winga, por me ensinares que a música é a sincronia que se gera sem serem necessárias palavras. Obrigada pela paciência e cumplicidade, por todas as vezes em que conseguiste aligeirar o peso de um dia menos bom e ajudar-me a encontrar motivação para continuar a manter o ritmo.

À minha família, pelo apoio incondicional e por me proporcionarem a possibilidade de seguir aquilo que me fascina.

À minha mãe, meu eterno porto de abrigo, todas as palavras serão poucas. Obrigada por nunca me deixares desistir, inspirando-me desde sempre a fazer mais e melhor.

9 | REFERENCES

Almolda, B., de Labra, C., Barrera, I., Gruart, A., Delgado-Garcia, J. M., Villacampa, N., … Castellano, B. (2015). Alterations in microglial phenotype and hippocampal neuronal function in transgenic mice with astrocyte-targeted production of interleukin-10. *Brain, Behavior, and Immunity*, *45*, 80–97.

Arendash, G. W., Mori, T., Cao, C., Mamcarz, M., Runfeldt, M., Dickson, A., … Potter, H. (2009). Caffeine reverses cognitive impairment and decreases brain amyloid-beta levels in aged Alzheimer's disease mice. *Journal of Alzheimer's Disease: JAD*, *17*, 661–680.

Banasr, M., & Duman, R. S. (2007). Regulation of neurogenesis and gliogenesis by stress and antidepressant treatment. *CNS & Neurological Disorders Drug Targets*, *6*, 311–320.

Batalha, V. L., Pego, J. M., Fontinha, B. M., Costenla, A. R., Valadas, J. S., Baqi, Y., … Lopes, L. V. (2013). Adenosine A(2A) receptor blockade reverts hippocampal stress-induced deficits and restores corticosterone circadian oscillation. *Molecular Psychiatry*, *18*, 320–331.

Benarroch, E. E. (2010). Glutamate transporters: diversity, function, and involvement in neurologic disease. *Neurology*, *74*, 259–264.

Biber, K., Neumann, H., Inoue, K., & Boddeke, H. W. G. M. (2007). Neuronal "On" and "Off" signals control microglia. *Trends in Neurosciences*, *30*, 596–602.

Boison, D., Chen, J.-F., & Fredholm, B. B. (2010). Adenosine signaling and function in glial cells. *Cell Death and Differentiation*, *17*, 1071–1082.

Canas, P., Rebola, N., & Rodrigues, R. (2004). Increased adenosine A2A immunoreactivity in activated rat microglia in culture (Vol. A223.9). Presented at the 4th Forum of European Neuroscience.

Cardona, A. E., Pioro, E. P., Sasse, M. E., Kostenko, V., Cardona, S. M., Dijkstra, I. M., … Ransohoff, R. M. (2006). Control of microglial neurotoxicity by the fractalkine receptor. *Nature Neuroscience*, *9*, 917–924.

Coelho, J. E., Alves, P., Canas, P. M., Valadas, J. S., Shmidt, T., Batalha, V. L., … Lopes, L. V. (2014). Overexpression of Adenosine A2A Receptors in Rats: Effects on Depression, Locomotion, and Anxiety. *Frontiers in Psychiatry*, *5*, 67.

Cristóvão-Ferreira, S., Vaz, S. H., Ribeiro, J. A., & Sebastião, A. M. (2009). Adenosine A2A receptors enhance GABA transport into nerve terminals by restraining PKC inhibition of GAT-1. *Journal of Neurochemistry*, *109*, 336–347.

Cunha, R. A. (2005). Neuroprotection by adenosine in the brain: From A1 receptor activation to A2A receptor blockade. *Purinergic Signalling*, *1*, 111–134.

Cunha, R. A., & Ribeiro, J. A. (2000). Adenosine A2A receptor facilitation of synaptic transmission in the CA1 area of the rat hippocampus requires protein kinase C but not protein kinase A activation. *Neuroscience Letters*, *289*, 127–130.

Dai, S. S., Zhou, Y. G., Li, W., An, J. H., Li, P., Yang, N., … Chen, J. F. (2010). Local Glutamate Level Dictates Adenosine A2A Receptor Regulation of Neuroinflammation and Traumatic Brain Injury. *Journal of Neuroscience*, *30*, 5802–5810.

Daré, E., Schulte, G., Karovic, O., Hammarberg, C., & Fredholm, B. B. (2007). Modulation of glial cell functions by adenosine receptors. *Physiology & Behavior*, *92*, 15–20.

Das Sarma, S., Chatterjee, K., Dinda, H., Chatterjee, D., & Das Sarma, J. (2013). Cytomorphological and Cytochemical Identification of Microglia. *ISRN Immunology*, *2013*, 1–10.

Diógenes, M. J., Costenla, A. R., Lopes, L. V., Jerónimo-Santos, A., Sousa, V. C., Fontinha, B. M., … Sebastião, A. M. (2011). Enhancement of LTP in Aged Rats is Dependent on Endogenous BDNF. *Neuropsychopharmacology*, *36*, 1823–1836.

Doorn, K. J., BrevÃ©, J. J. P., Drukarch, B., Boddeke, H. W., Huitinga, I., Lucassen, P. J., & van Dam, A.-M. (2015). Brain region-specific gene expression profiles in freshly isolated rat microglia. *Frontiers in Cellular Neuroscience*, *9*. doi:10.3389/fncel.2015.00084

Eng, L. F., Ghirnikar, R. S., & Lee, Y. L. (2000). Glial fibrillary acidic protein: GFAP-thirty-one years (1969-2000). *Neurochemical Research*, *25*, 1439–1451.

Ferreira, D. G., Batalha, V. L., Vicente Miranda, H., Coelho, J. E., Gomes, R., Gonçalves, F. Q., … Lopes, L. V. (2015). Adenosine A2A Receptors Modulate α-Synuclein Aggregation and Toxicity. *Cerebral Cortex (New York, N.Y.: 1991)*. doi:10.1093/cercor/bhv268

Ford, A. L., Goodsall, A. L., Hickey, W. F., & Sedgwick, J. D. (1995). Normal adult ramified microglia separated from other central nervous system macrophages by flow cytometric sorting. Phenotypic differences defined and direct ex vivo antigen presentation to myelin basic protein-reactive CD4+ T cells compared. *Journal of Immunology (Baltimore, Md.: 1950)*, *154*, 4309–4321.

Fredholm, B. B., Chen, J.-F., Cunha, R. A., Svenningsson, P., & Vaugeois, J.-M. (2005). Adenosine and brain function. *International Review of Neurobiology*, *63*, 191–270.

Fredholm, B. B., Chern, Y., Franco, R., & Sitkovsky, M. (2007). Aspects of the general biology of adenosine A2A signaling. *Progress in Neurobiology*, *83*, 263–276.

Gao, Z., & Tsirka, S. E. (2011). Animal Models of MS Reveal Multiple Roles of Microglia in Disease Pathogenesis. *Neurology Research International*, *2011*, 383087.

Giménez-Llort, L., Schiffmann, S. N., Shmidt, T., Canela, L., Camón, L., Wassholm, M., … Bader, M. (2007). Working memory deficits in transgenic rats overexpressing human adenosine A2A receptors in the brain. *Neurobiology of Learning and Memory*, *87*, 42–56.

González-Scarano, F., & Baltuch, G. (1999). Microglia as mediators of inflammatory and degenerative diseases. *Annual Review of Neuroscience*, *22*, 219–240.

Gosselin, R.-D., Gibney, S., O'Malley, D., Dinan, T. G., & Cryan, J. F. (2009). Region specific decrease in glial fibrillary acidic protein immunoreactivity in the brain of a rat model of depression. *Neuroscience*, *159*, 915–925.

Gyoneva, S., Shapiro, L., Lazo, C., Garnier-Amblard, E., Smith, Y., Miller, G. W., & Traynelis, S. F. (2014). Adenosine A2A receptor antagonism reverses inflammation-induced impairment of microglial process extension in a model of Parkinson's disease. *Neurobiology of Disease*, *67*, 191–202.

Hayashi, Y., Ishibashi, H., Hashimoto, K., & Nakanishi, H. (2006). Potentiation of the NMDA receptor-mediated responses through the activation of the glycine site by microglia secreting soluble factors. *Glia*, *53*, 660–668.

Hodel, A. (1998). SNAP-25. *The International Journal of Biochemistry & Cell Biology*, *30*, 1069–1073.

Hooper, C., & Pocock, J. (2015, October 27). An overview of microglia subtypes and markers. Retrieved from http://www.abcam.com/neuroscience/an-overview-of-microglia-subtypes-and-markers

Hughes, E. G., Maguire, J. L., McMinn, M. T., Scholz, R. E., & Sutherland, M. L. (2004). Loss of glial fibrillary acidic protein results in decreased glutamate transport and inhibition of PKA-induced EAAT2 cell surface trafficking. *Molecular Brain Research*, *124*, 114–123.

Hu, X., Li, P., Guo, Y., Wang, H., Leak, R. K., Chen, S., … Chen, J. (2012). Microglia/Macrophage Polarization Dynamics Reveal Novel Mechanism of Injury Expansion After Focal Cerebral Ischemia. *Stroke*, *43*, 3063–3070.

Imbe, H., Kimura, A., Donishi, T., & Kaneoke, Y. (2012). Chronic restraint stress decreases glial fibrillary acidic protein and glutamate transporter in the periaqueductal gray matter. *Neuroscience*, *223*, 209–218.

Ito, D., Tanaka, K., Suzuki, S., Dembo, T., & Fukuuchi, Y. (2001). Enhanced expression of Iba1, ionized calcium-binding adapter molecule 1, after transient focal cerebral ischemia in rat brain. *Stroke; a Journal of Cerebral Circulation*, *32*, 1208–1215.

Jeong, H.-K., Ji, K., Min, K., & Joe, E.-H. (2013). Brain Inflammation and Microglia: Facts and Misconceptions. *Experimental Neurobiology*, *22*, 59.

Ji, K., Miyauchi, J., & Tsirka, S. E. (2013). Microglia: an active player in the regulation of synaptic activity. *Neural Plasticity*, *2013*, 627325.

Kanazawa, H., Ohsawa, K., Sasaki, Y., Kohsaka, S., & Imai, Y. (2002). Macrophage/microglia-specific protein Iba1 enhances membrane ruffling and Rac activation via phospholipase C-gamma -dependent pathway. *The Journal of Biological Chemistry*, *277*, 20026–20032.

Kay, A. R., & Wong, R. K. (1986). Isolation of neurons suitable for patch-clamping from adult mammalian central nervous systems. *Journal of Neuroscience Methods*, *16*, 227–238.

Kettenmann, H., Hanisch, U.-K., Noda, M., & Verkhratsky, A. (2011). Physiology of Microglia. *Physiological Reviews*, *91*, 461–553.

Kettenmann, H., & Verkhratsky, A. (2011). Neuroglia, der lebende Nervenkitt. *Fortschritte der Neurologie · Psychiatrie*, *79*, 588–597.

Khoa, N. D., Postow, M., Danielsson, J., & Cronstein, B. N. (2006). Tumor necrosis factor-alpha prevents desensitization of Galphas-coupled receptors by regulating GRK2 association with the plasma membrane. *Molecular Pharmacology*, *69*, 1311–1319.

Kumar, A., Stoica, B. A., Sabirzhanov, B., Burns, M. P., Faden, A. I., & Loane, D. J. (2013). Traumatic brain injury in aged animals increases lesion size and chronically alters microglial/macrophage classical and alternative activation states. *Neurobiology of Aging*, *34*, 1397–1411.

Laurent, C., Burnouf, S., Ferry, B., Batalha, V. L., Coelho, J. E., Baqi, Y., … Blum, D. (2016). A2A adenosine receptor deletion is protective in a mouse model of Tauopathy. *Molecular Psychiatry*, *21*, 97–107.

Lawson, L. J., Perry, V. H., & Gordon, S. (1992). Turnover of resident microglia in the normal adult mouse brain. *Neuroscience*, *48*, 405–415.

Lee, F. S., & Chao, M. V. (2001). Activation of Trk neurotrophin receptors in the absence of neurotrophins. *Proceedings of the National Academy of Sciences of the United States of America*, *98*, 3555–3560.

Liao, B., Zhao, W., Beers, D. R., Henkel, J. S., & Appel, S. H. (2012). Transformation from a neuroprotective to a neurotoxic microglial phenotype in a mouse model of ALS. *Experimental Neurology*, *237*, 147–152.

Lopes, L. V., Cunha, R. A., Kull, B., Fredholm, B. B., & Ribeiro, J. A. (2002). Adenosine A(2A) receptor facilitation of hippocampal synaptic transmission is dependent on tonic A(1) receptor inhibition. *Neuroscience*, *112*, 319–329.

Lopes, L. V., Cunha, R. A., & Ribeiro, J. A. (1999). Increase in the number, G protein coupling, and efficiency of facilitatory adenosine A2A receptors in the limbic cortex, but not striatum, of aged rats. *Journal of Neurochemistry*, *73*, 1733–1738.

Lucin, K. M., & Wyss-Coray, T. (2009). Immune Activation in Brain Aging and Neurodegeneration: Too Much or Too Little? *Neuron*, *64*, 110–122.

Magistretti, P., & Ransom, B. (2002). Astrocytes. In K. David, D. Charney, J. Coyle, & C. Nemeroff (Eds.), *Neuropsychopharmacology: The Fifth Generation of Progress* (pp. 133–145). American College of Neuropsychopharmacology.

Malek, R. L., Nie, Z., Ramkumar, V., & Lee, N. H. (1999). Adenosine A(2A) receptor mRNA regulation by nerve growth factor is TrkA-, Src-, and Ras-dependent via extracellular regulated kinase and stress-activated protein kinase/c-Jun NH(2)-terminal kinase. *The Journal of Biological Chemistry*, *274*, 35499–35504.

Mandrekar-Colucci, S., Karlo, J. C., & Landreth, G. E. (2012). Mechanisms underlying the rapid peroxisome proliferator-activated receptor-γ-mediated amyloid clearance and reversal of cognitive deficits in a murine model of Alzheimer's disease. *The Journal of Neuroscience: The Official Journal of the Society for Neuroscience*, *32*, 10117–10128.

Maragakis, N. J., & Rothstein, J. D. (2006). Mechanisms of Disease: astrocytes in neurodegenerative disease. *Nature Clinical Practice Neurology*, *2*, 679–689.

Marcoli, M., Raiteri, L., Bonfanti, A., Monopoli, A., Ongini, E., Raiteri, M., & Maura, G. (2003). Sensitivity to selective adenosine A1 and A2A receptor antagonists of the release of glutamate induced by ischemia in rat cerebrocortical slices. *Neuropharmacology*, *45*, 201–210.

Matos, M., Augusto, E., Santos-Rodrigues, A. D., Schwarzschild, M. A., Chen, J.-F., Cunha, R. A., & Agostinho, P. (2012). Adenosine A2A receptors modulate glutamate uptake in cultured astrocytes and gliosomes. *Glia*, *60*, 702–716.

McGeer, P. L., Itagaki, S., Boyes, B. E., & McGeer, E. G. (1988). Reactive microglia are positive for HLA-DR in the substantia nigra of Parkinson's and Alzheimer's disease brains. *Neurology*, *38*, 1285–1291.

McGeer, P. L., Itagaki, S., Tago, H., & McGeer, E. G. (1987). Reactive microglia in patients with senile dementia of the Alzheimer type are positive for the histocompatibility glycoprotein HLA-DR. *Neuroscience Letters*, *79*, 195–200.

Mikita, J., Dubourdieu-Cassagno, N., Deloire, M. S., Vekris, A., Biran, M., Raffard, G., … Petry, K. G. (2011). Altered M1/M2 activation patterns of monocytes in severe relapsing experimental rat model of multiple

sclerosis. Amelioration of clinical status by M2 activated monocyte administration. *Multiple Sclerosis (Houndmills, Basingstoke, England)*, *17*, 2–15.

Morel, G. R., Andersen, T., Pardo, J., Zuccolilli, G. O., Cambiaggi, V. L., Hereñú, C. B., & Goya, R. G. (2015). Cognitive impairment and morphological changes in the dorsal hippocampus of very old female rats. *Neuroscience*, *303*, 189–199.

Moriguchi, S., Mizoguchi, Y., Tomimatsu, Y., Hayashi, Y., Kadowaki, T., Kagamiishi, Y., … Nakanishi, H. (2003). Potentiation of NMDA receptor-mediated synaptic responses by microglia. *Brain Research. Molecular Brain Research*, *119*, 160–169.

Nisticò, R., Mango, D., Mandolesi, G., Piccinin, S., Berretta, N., Pignatelli, M., … Centonze, D. (2013). Inflammation Subverts Hippocampal Synaptic Plasticity in Experimental Multiple Sclerosis. *PLoS ONE*, *8*, e54666.

Oberheim, N. A., Goldman, S. A., & Nedergaard, M. (2012). Heterogeneity of Astrocytic Form and Function. In R. Milner (Ed.), *Astrocytes* (Vol. 814, pp. 23–45). Totowa, NJ: Humana Press.

Olah, M., Biber, K., Vinet, J., & W.G.M. Boddeke, H. (2011). Microglia Phenotype Diversity. *CNS & Neurological Disorders - Drug Targets*, *10*, 108–118.

Orr, A. G., Hsiao, E. C., Wang, M. M., Ho, K., Kim, D. H., Wang, X., … Mucke, L. (2015). Astrocytic adenosine receptor A2A and Gs-coupled signaling regulate memory. *Nature Neuroscience*, *18*, 423–434.

Orr, A. G., Orr, A. L., Li, X.-J., Gross, R. E., & Traynelis, S. F. (2009). Adenosine A2A receptor mediates microglial process retraction. *Nature Neuroscience*, *12*, 872–878.

Pascual, O., Ben Achour, S., Rostaing, P., Triller, A., & Bessis, A. (2012). Microglia activation triggers astrocyte-mediated modulation of excitatory neurotransmission. *Proceedings of the National Academy of Sciences of the United States of America*, *109*, E197–205.

Pedersen, W. A., Wan, R., Zhang, P., & Mattson, M. P. (2002). Urocortin, but not urocortin II, protects cultured hippocampal neurons from oxidative and excitotoxic cell death via corticotropin-releasing hormone receptor type I. *The Journal of Neuroscience: The Official Journal of the Society for Neuroscience*, *22*, 404–412.

Pekny, M., Pekna, M., Messing, A., Steinhäuser, C., Lee, J.-M., Parpura, V., … Verkhratsky, A. (2016). Astrocytes: a central element in neurological diseases. *Acta Neuropathologica*, *131*, 323–345.

Pocock, J. M., & Kettenmann, H. (2007). Neurotransmitter receptors on microglia. *Trends in Neurosciences*, *30*, 527–535.

Rebola, N., Oliveira, C. R., & Cunha, R. A. (2002). Transducing system operated by adenosine A(2A) receptors to facilitate acetylcholine release in the rat hippocampus. *European Journal of Pharmacology*, *454*, 31–38.

Rebola, N., Simões, A. P., Canas, P. M., Tomé, A. R., Andrade, G. M., Barry, C. E., … Cunha, R. A. (2011). Adenosine A2A receptors control neuroinflammation and consequent hippocampal neuronal dysfunction: A2A receptors control neuroinflammation. *Journal of Neurochemistry*, *117*, 100–111.

Ribeiro, J. A., & Sebastião, A. M. (2010). Modulation and metamodulation of synapses by adenosine: Adenosine modulation and metamodulation. *Acta Physiologica*, *199*, 161–169.

Ribeiro, J. A., Sebastiao, A. M., & de Mendonca, A. (2003). Participation of adenosine receptors in neuroprotection. *Drug News & Perspectives*, *16*, 80–86.

Rodríguez-Arellano, J. J., Parpura, V., Zorec, R., & Verkhratsky, A. (2015). Astrocytes in physiological aging and Alzheimer's disease. *Neuroscience*. doi:10.1016/j.neuroscience.2015.01.007

Rosenzweig, E. S., & Barnes, C. A. (2003). Impact of aging on hippocampal function: plasticity, network dynamics, and cognition. *Progress in Neurobiology*, *69*, 143–179.

Roy, A., Fung, Y. K., Liu, X., & Pahan, K. (2006). Up-regulation of Microglial CD11b Expression by Nitric Oxide. *Journal of Biological Chemistry*, *281*, 14971–14980.

Santiago, A. R., Baptista, F. I., Santos, P. F., Cristóvão, G., Ambrósio, A. F., Cunha, R. A., & Gomes, C. A. (2014). Role of Microglia Adenosine A $_{2A}$ Receptors in Retinal and Brain Neurodegenerative Diseases. *Mediators of Inflammation*, *2014*, 1–13.

Schafer, D. P., Lehrman, E. K., & Stevens, B. (2013). The "quad-partite" synapse: Microglia-synapse interactions in the developing and mature CNS. *Glia*, *61*, 24–36.

Schulte, G., & Fredholm, B. B. (2003). Signalling from adenosine receptors to mitogen-activated protein kinases. *Cellular Signalling*, *15*, 813–827.

Sebastiao, A., & Ribeiro, J. (2009). Tuning and Fine-Tuning of Synapses with Adenosine. *Current Neuropharmacology*, *7*, 180–194.

Sedgwick, J. D., Schwender, S., Imrich, H., Dörries, R., Butcher, G. W., & ter Meulen, V. (1991). Isolation and direct characterization of resident microglial cells from the normal and inflamed central nervous system. *Proceedings of the National Academy of Sciences of the United States of America*, *88*, 7438–7442.

Shechter, R., & Schwartz, M. (2013). Harnessing monocyte-derived macrophages to control central nervous system pathologies: no longer “if” but “how”: Macrophages beyond inflammation in CNS pathologies. *The Journal of Pathology*, *229*, 332–346.

Simões, A., Duarte, J. A., Agasse, F., Canas, P., Tomé, A. R., Agostinho, P., & Cunha, R. A. (2012). Blockade of adenosine A2A receptors prevents interleukin-1β-induced exacerbation of neuronal toxicity through a p38 mitogen-activated protein kinase pathway. *Journal of Neuroinflammation*, *9*, 204.

Si, X., Miguel-Hidalgo, J. J., O’Dwyer, G., Stockmeier, C. A., & Rajkowska, G. (2004). Age-Dependent Reductions in the Level of Glial Fibrillary Acidic Protein in the Prefrontal Cortex in Major Depression. *Neuropsychopharmacology*, *29*, 2088–2096.

Sofroniew, M. V., & Vinters, H. V. (2010). Astrocytes: biology and pathology. *Acta Neuropathologica*, *119*, 7–35.

Stathakis, D. G., Hoover, K. B., You, Z., & Bryant, P. J. (1997). Human postsynaptic density-95 (PSD-95): location of the gene (DLG4) and possible function in nonneural as well as in neural tissues. *Genomics*, *44*, 71–82.

Stehberg, J., Moraga-Amaro, R., Salazar, C., Becerra, A., Echeverría, C., Orellana, J. A., … Retamal, M. A. (2012). Release of gliotransmitters through astroglial connexin 43 hemichannels is necessary for fear memory consolidation in the basolateral amygdala. *FASEB Journal: Official Publication of the Federation of American Societies for Experimental Biology*, *26*, 3649–3657.

Stellwagen, D., & Malenka, R. C. (2006). Synaptic scaling mediated by glial TNF-alpha. *Nature*, *440*, 1054–1059.

Su, X., Maguire-Zeiss, K. A., Giuliano, R., Prifti, L., Venkatesh, K., & Federoff, H. J. (2008). Synuclein activates microglia in a model of Parkinson’s disease. *Neurobiology of Aging*, *29*, 1690–1701.

Tambuyzer, B. R., Ponsaerts, P., & Nouwen, E. J. (2009). Microglia: gatekeepers of central nervous system immunology. *Journal of Leukocyte Biology*, *85*, 352–370.

Tebano, M. T., Martire, A., Pepponi, R., Domenici, M. R., & Popoli, P. (2006). Is the functional interaction between adenosine A(2A) receptors and metabotropic glutamate 5 receptors a general mechanism in the brain? Differences and similarities between the striatum and the hippocampus. *Purinergic Signalling*, *2*, 619–625.

Temido-Ferreira, M., Coelho, J. E., Ferreira, D. G., Outeiro, T. F., Bader, M., Marie, H., … Lopes, L. V. (2015). Neuronal Adenosine A2A Receptor Overexpression affects AMPA and NMDA currents in CA1

hippocampal neurons. Presented at the 45th Annual Meeting of the Society for Neurocience, Chicago, U.S.A.

Towbin, H., Staehelin, T., & Gordon, J. (1979). Electrophoretic transfer of proteins from polyacrylamide gels to nitrocellulose sheets: procedure and some applications. *Proceedings of the National Academy of Sciences of the United States of America*, *76*, 4350–4354.

Tynan, R. J., Beynon, S. B., Hinwood, M., Johnson, S. J., Nilsson, M., Woods, J. J., & Walker, F. R. (2013). Chronic stress-induced disruption of the astrocyte network is driven by structural atrophy and not loss of astrocytes. *Acta Neuropathologica*, *126*, 75–91.

Verkhratsky, A., Marutle, A., Rodriguez-Arellano, J. J., & Nordberg, A. (2015). Glial Asthenia and Functional Paralysis: A New Perspective on Neurodegeneration and Alzheimer's Disease. *The Neuroscientist*, *21*, 552–568.

Wu, M., Nissen, J. C., Chen, E. I., & Tsirka, S. E. (2012). Tuftsin promotes an anti-inflammatory switch and attenuates symptoms in experimental autoimmune encephalomyelitis. *PloS One*, *7*, e34933.

Ye, Y., Wang, G., Wang, H., & Wang, X. (2011). Brain-derived neurotrophic factor (BDNF) infusion restored astrocytic plasticity in the hippocampus of a rat model of depression. *Neuroscience Letters*, *503*, 15–19.

Yu, L., Shen, H.-Y., Coelho, J. E., Araújo, I. M., Huang, Q.-Y., Day, Y.-J., … Chen, J.-F. (2008). Adenosine A $_{2A}$ receptor antagonists exert motor and neuroprotective effects by distinct cellular mechanisms. *Annals of Neurology*, *63*, 338–346.